O. S. Wolfbeis et al.

DOI: 10.1002/anie.201307828

Sensor Materials

Photonic Crystals for Chemical Sensing and Biosensing

*Christoph Fenzl, Thomas Hirsch, and Otto S. Wolfbeis**

Keywords:
analytical methods · biosensors · chemical sensor · structural color · photonic crystals

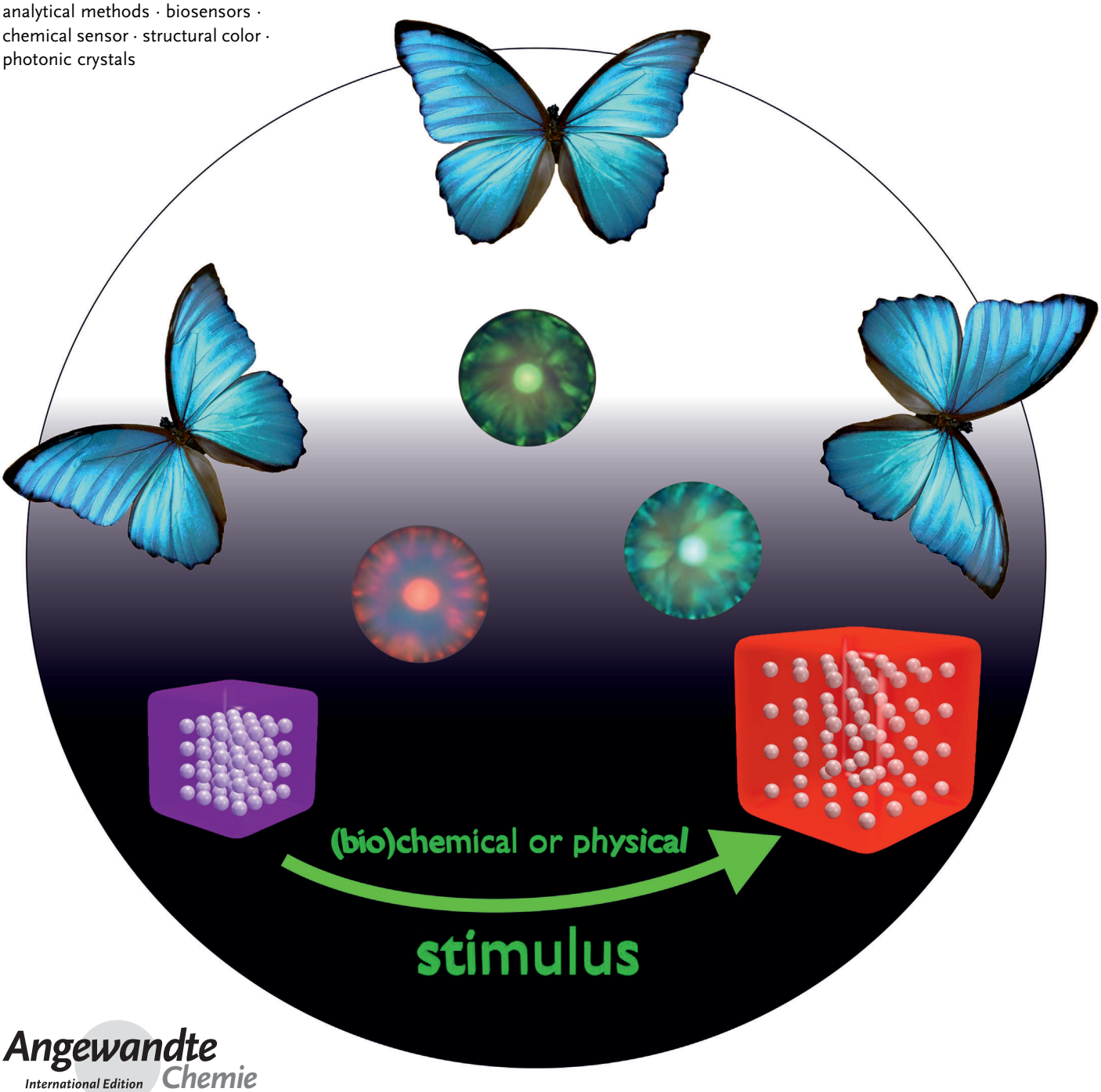

Angewandte International Edition Chemie

This Review covers photonic crystals (PhCs) and their use for sensing mainly chemical and biochemical parameters, with a particular focus on the materials applied. Specific sections are devoted to a) a lead-in into natural and synthetic photonic nanoarchitectures, b) the various kinds of structures of PhCs, c) reflection and diffraction in PhCs, d) aspects of sensing based on mechanical, thermal, optical, electrical, magnetic, and purely chemical stimuli, e) aspects of biosensing based on biomolecules incorporated into PhCs, and f) current trends and limitations of such sensors.

From the Contents

1. Introduction: Natural and Synthetic Photonic Nanoarchitectures

Nature provides a large variety of shapes and colors in living creatures. It makes use of many approaches to produce its colorful kaleidoscope, the most common methods being coloration by pigments, dyes, or structure. Although pigments and dyes owe their color to the absorption of light, structural color has its origin in geometric structures capable of manipulating the diffraction and/or reflection of light through periodically arranged photonic nanostructures. Usually, this form of color generation is more efficient. Insects, unlike plants, widely use this principle.

Photonic crystals (PhCs) can be considered as periodic arrangements of regularly shaped materials (often a multiplicity of layers or spheres in a host polymer) with different dielectric constants. Periodicity can vary from single-dimensional (1D) to three-dimensional (3D). PhCs have distinct wavelengths of reflection that are governed by the distance between the layers or spheres, and this causes their specific color. If the periodicity of the crystal is changed, for example, by a (bio)chemical stimulus, the wavelength of maximum reflectance also will change. Hence, the effect offers a convenient tool for sensing, in particular if the effect can be made specific for the stimulus. Such effects also are even amenable to visual readout by unskilled operators. Moreover, methods are likely to be cheap, and handling is fairly easy. Some of these features make them more attractive than other kinds of stimuli-responsive materials.[1] It therefore does not come as a surprise that such color changes have become the basis for a variety of physical, chemical, and biological sensors.

2. Fundamentals of Photonic Crystals

Nature uses photonic crystals (PhCs) to a wide extent.[2] Animals such as certain butterflies and beetles use them for mimicry and survival techniques, for example, to distract predators.[3–5] The periodicity of the nanostructures ranges from one- to three-dimensional and can be found in a large variety of living species of higher order.[6–13] Butterflies (such as *Morpho rhetenor*) are the organisms most commonly referred to in order to illustrate this effect (Figure 1). Such periodic structures can not only exhibit many hues of color, but can also change on application of an external stimulus, which leads to an alternation of color.

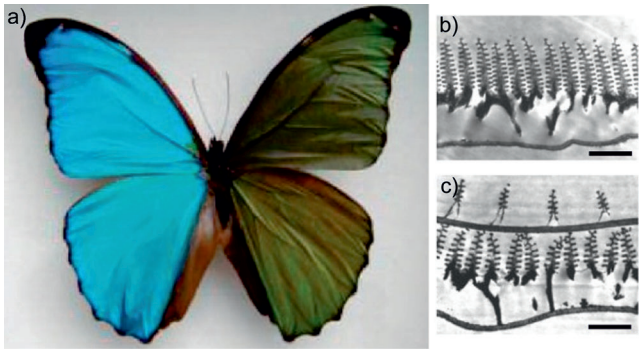

Figure 1. a) Photography of the wings of *Morpho rhetenor* after ethanol was poured over the right wing; b) transmission electron microscopy (TEM) image of the cross-section of its wing scales; c) TEM image of the cross-section of the wing scales of the related species *Morpho didius*. Scale bars are 1.8 μm in (b) and 1.3 μm in (c). Figure (a) adapted from Ref. [5] with permission; copyright 2009 American Chemical Society. Pictures (b) and (c) reprinted from Ref. [3]; copyright 2003 Macmillan Publishers Ltd.

[*] M. Sc. C. Fenzl, Dr. T. Hirsch, Prof. O. S. Wolfbeis
Institut für Analytische Chemie, Chemo- und Biosensorik
Universität Regensburg
93040 Regensburg (Germany)
E-mail: otto.wolfbeis@ur.de
Homepage: http://www.wolfbeis.de

From a physical point of view, PhCs can be described as a periodic arrangement of regularly shaped, mostly transparent materials with different dielectric constants. The material is engineered such that only light of a certain wavelength can propagate through the lattice of this arrangement.[14] Yablonovitch and John performed the first detailed research on engineered PhCs.[15,16] Three kinds of structures of PhCs may be discerned (Figure 2).

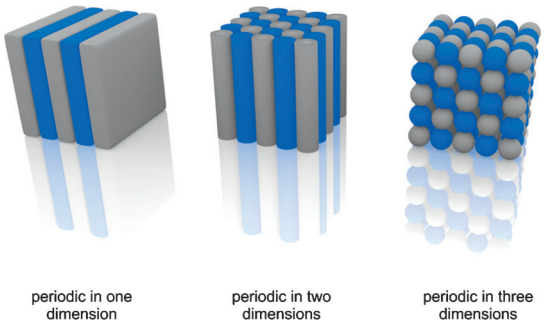

Figure 2. Schematic representation of the three kinds of photonic crystals. The different colors represent materials with different dielectric constants. In 2D or 3D PhCs the structure can also be formed by a single material with the correct distance between each element.

One-dimensional PhCs are the simplest variation, where the periodicity exists in only one dimension. These are also known as Bragg reflectors or Bragg stacks, which reflect one specific wavelength and usually have a smooth surface like a mirror. They are typically produced by techniques such as layer-by-layer deposition, multiple spin coating, or photolithography.[17–19] Two-dimensional photonic crystals are characterized by their periodicity in two spatial directions.[20] They are primarily produced by complex top-down methods such as photolithography and etching techniques.[21] The nanostructures can be varied in form, order, size, and defects to manipulate their properties.[22–25] The Asher research group has recently studied responsive 2D arrays on a hydrogel support/matrix for use in sensing. Such studies include the vertical spreading of 2D crystalline colloidal arrays (CCAs),[26] 2D array Debye ring diffraction for protein recognition,[27] the simulation of the Langevin dynamics of 3D colloidal crystal vacancies and phase transitions,[28] the fabrication of large-area 2D colloidal crystals,[20] and the enhancement of the reflectivity of the monolayer diffraction in a 2D dielectric particle array.[29]

Three-dimensional (3D) PhCs display periodicity in three dimensions.[30,31] Examples of common 3D structures are opals[9] and inverse opals.[32] These terms originate from a class of minerals that shows such a periodic 3D arrangement. Although there are several different top-down approaches to produce 3D photonic crystals,[33–37] chemical bottom-up methods are now more simple and cheaper.[38–41] The primary method used is based on the self-assembly of nanoscopic, monodisperse spheres into a photonic crystal host.[9,42] Typically, such spheres consist of silica, zinc oxide, titanium dioxide, or organic polymers such as polystyrene or poly(methyl methacrylate).[21,43–49] Early studies on diffraction in CCAs have corroborated particularly efficient diffraction in monodisperse polystyrene colloids,[50] and on colloidal Bragg diffraction devices that form the basis of a new generation of Raman spectrometers.[51] Common methods for assembly that lead to a 3D arrangement utilize particle properties such as electrostatic repulsion or magnetism as well as inertial forces and capillary interactions.[38,52,53]

3. Reflection in Photonic Crystals

The well-known phenomenon of X-ray diffraction is presented schematically in Figure 3. This model can also explain how photonic crystals reflect light of certain wavelengths. X-ray diffraction theory assumes regularly arranged atoms placed in a vacuum. Bragg's law of diffraction describes

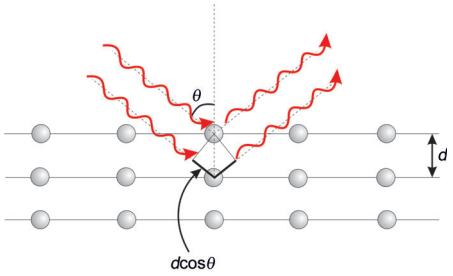

Figure 3. Simplified scheme of light reflection from ordered spheres by analogy to the explanation of X-ray diffraction.

Christoph Fenzl received his BSc and MSc in chemistry from the University of Regensburg in 2010 and 2012, respectively. He was a scholarship member of the German National Academic Foundation from 2008 to 2012 and received several awards from the university and the German Chemical Society for being the best BSc and MSc student of the year. He is now carrying out PhD research, and has spent 3 months at Cornell University with Prof. Baeumner. His research is focused on colloidal photonic crystals for use in chemical sensors and new sensor systems based on surface plasmon resonance.

Thomas Hirsch obtained his PhD from the University of Regensburg under the supervision of Prof. Otto S. Wolfbeis in 2008 and is now a lecturer at the Institute of Analytical Chemistry, Chemo-, and Biosensors at the University of Regensburg, Germany. His research interests include nanomaterials for sensor applications as well as self-assembly technologies. He has published over 20 papers on optical and electrochemical (bio)-sensors and on advanced nanomaterials.

constructive interference according to Equation (1), where d is the distance between atomic planes, θ is the angle of incident light, m is the order of diffraction, and λ is the wavelength of incident light.[54] A photonic crystal array consists of dielectric spheres within a dielectric medium such as air or solvent. Combining Bragg's law with Snell's law of refraction leads to Equation (2), where d is the distance between particle planes, n_{eff} is the mean effective refractive index (RI), θ is the angle of incident light, m is the order of reflection, and λ is the wavelength of the reflected light. The reflected wavelength can also be calculated using the center-to-center distance D between the particles. The application of this method leads to Equation (3). The mean effective refractive index n_{eff} is defined as Equation (4), where n_p and n_m are the refractive indices of the particles and surrounding medium, respectively, and V_p and V_m are the respective volume fractions.[55–57]

$$2\,d\cos\theta = m\lambda \tag{1}$$

$$2\,d(n_{eff}^2 - \sin^2\theta)^{1/2} = m\lambda \tag{2}$$

$$\sqrt{\frac{8}{3}}D(n_{eff}^2 - \sin^2\theta)^{1/2} = m\lambda \tag{3}$$

$$n_{eff}^2 = n_p^2 V_p + n_m^2 V_m \tag{4}$$

4. Aspects of Physical and Chemical Sensing

The phenomena described above can be applied to sensing[58] if the reflected wavelength can be altered by external (chemical) stimuli. For example, the wavelength of the reflected light will change when the angle of incidence (or the orientation of the crystal array) is altered. This variable can be used to verify the orientation of the PhC.[59,60] Distance and refractive index are two other variables that can cause a change in the reflected wavelength. Although both often vary simultaneously, the relative change in distance is usually much more significant than that of the refractive index.[2] However, sensors that utilize a change in the refractive index or an alteration of a single photonic unit cell may display higher sensitivity and faster response times.[61] The incorporation of photonic crystals into a polymer host such as a hydrogel represents one example that makes use of this basic principle (Figure 4).

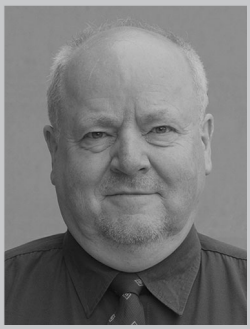

Otto S. Wolfbeis was a Full Professor of Analytical and Interface Chemistry at the University of Regensburg from 1995 to 2012. He has authored numerous papers and reviews on chemical sensors, fluorescent probes, labels and bioassays, on advanced (nano)materials for use in sensing schemes, and on methods in fluorescence and fluorescent imaging. He has (co)edited several books, and has acted as the (co)organizer of several conferences related to fluorescence spectroscopy (MAF) and to chemical sensors and biosensors (Europtrode). He is a Board Member of Angewandte Chemie.

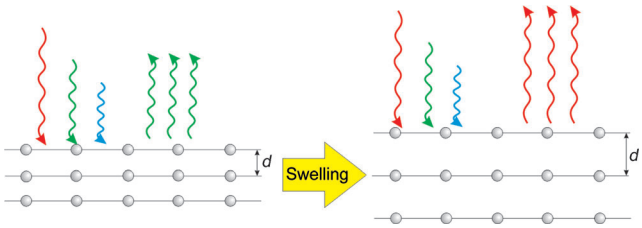

Figure 4. Response of a PhC sensor based on a swelling polymer.

With the initial distance between the particles fixed in a polymer, changes in wavelength will occur on either swelling or shrinking of the host matrix.[62] However, care has to be taken not to change the geometrical angle while varying the parameters. The challenge is to make this process selectively responsive for certain physical or chemical stimuli. This Review focuses on sensors based on photonic crystals that respond to certain physicochemical and chemical stimuli. It does not cover sensors that make use of photonic crystal fibers or waveguides as signal transducing devices.[63,64]

5. Types of Photonic Crystal Sensors

There are three major types of PhC sensors based on the use of the above materials, namely a) on-chip nanoscale resonators or waveguides, b) Bragg stacks made of mesoporous PhCs, and c) colloidally templated 3D PhCs. The on-chip nanoscale resonators or waveguides (see, for example, studies by the research groups of Erickson,[65] Arnold and Vollmer,[66] Armani and Vahala,[67] Loncar and Scherer,[68] Baba,[69] and Krauss[22]) are generally actuated by either changes in the local refractive index surrounding the cavities, or by adsorption of proteins. They possess several advantages:

1) Their small mode volume and sensor footprint allow small molecules (such as single proteins) to induce measurable changes in the cavity resonance, and also enable many sensors to be integrated into a single, CMOS-compatible chip. This makes this type of sensor attractive for multiplexed bioassays and chemical analytical methods that use a combinatorial approach.
2) PhC cavities tend to have much smaller line widths, that is, higher quality factors (Q factors) than typical Bragg reflection peaks (e.g. from a colloidal PhC sensor). This implies that very small perturbations can be detected (e.g. single proteins or very small changes in refractive index), thereby enhancing the sensitivity of the sensors.
3) Large-scale fabrication is often compatible with the CMOS technique, thereby potentially allowing easy integration of this type of sensor into consumer electronics.

The main disadvantages of this kind of sensor include the cost, power, and complexity of the readout. Read out is generally accomplished either with a tunable laser and a photodetector, or with a broadband telecom source and a grating spectrometer. These elements are more difficult to integrate while maintaining the performance, and certainly

place a lower limit on the cost and power requirements of a sensor. This is a disadvantage compared to colorimetric (or visual readout) sensors, for example. Another limitation is the freedom of material choice. High Q factor/volume cavities generally require precise nanofabrication, for which a limited number of materials are suited.

The Bragg stacks made of, for example, mesoporous silicon/silica/titania represent the second type of PhC sensors. Similar to the resonators described above, this type of PhC is generally actuated through the adsorption of material in the pores, as shown in studies by the research groups of Sailor,[70] Ozin,[71] Miguez,[72] and others. Their major advantage is the small size of the pores, which enables such sensors to gain specificity and sensitivity compared to simple refractive index sensors. This aspect is achieved through a couple of mechanisms: a) for larger molecules (e.g. biomolecules), the size of the pores can actually be tuned to filter for specific analytes. For example, Sailor and co-workers[70] used this effect to quantify protease activity in porous silicon photonic crystals; b) for smaller molecules, mesoporous materials can have sufficiently small pores and high porosity so that single-layer adsorption creates a large (even colorimetrically measurable) change in the effective refractive index. This allows the use of selective adsorption, rather than only differences in the refractive index of the adsorbing material. Ozin and co-workers[71] were able to make a highly specific photonic nose by using an array of mesoporous Bragg stacks functionalized with different surface groups that selectively adsorbed various vapors to different degrees. Its disadvantages include, again, a limited choice of available materials compared to colloidal PhCs, but certainly greater than that for integrated resonators, and colorimetric readout methods have been developed albeit in a trade-off with sensitivity, since broad peaks are typically being actuated and large shifts (30–50 nm) are required for visible color change. Potyrailo et al.[73] have estimated that this limits the sensitivity for gases to partial pressures of $p/p_0 \approx 0.1$ or greater for colorimetric readouts. On the other hand, even when spectroscopic readouts are used, they can be made at a lower cost than for integrated resonators with high Q factors (e.g. by using RGB outputs from a camera, as shown by Bonifacio et al.).[71]

Colloidally templated 3D photonic crystals (e.g. opals or inverse opals as demonstrated, for example in studies by the research groups of Asher,[74–76] Gu,[5,77–79] Stein,[48,57] Braun,[56] Xia,[55,80,81] and ourselves[82,83]) form the third main group. This type of sensor is most important in the context of this Review. Such PhC sensors possess the advantages of enabling many types of materials to be incorporated into the structure, and of many different sensing mechanisms to be used (including changes in refractive index resulting from pore filling, polymer/hydrogel swelling by liquids, and changes induced by physical stimuli (e.g. strain, electric fields, magnetic fields)). Other advantages include scalability (lowering costs of fabrication) and the prospect for power-free colorimetric detection. However, just like the mesoporous PhCs, colorimetric detection requires large resonance shifts and thus limits the sensitivity of many of the targeted sensing mechanisms.

6. Responsive Photonic Crystals

6.1. Mechanically Responsive Photonic Crystals

The simplest types of tunable PhCs are those that respond to mechanical stress, such as stretching or compression.[84–86] Asher et al. described a composite film consisting of polystyrene colloids embedded in an *N*-vinylpyrrolidone/acrylamide copolymer. The reflected wavelength maximum shifts from 573 to 538 nm after uniaxial stretching as a result of the reduction in the distance between the particles in the lattice.[87] Other matrix materials such as poly(methyl acrylate) and poly(ethylene glycol methacrylate) (PEGMA) were used to improve the stability. A wavelength shift of 55 nm is observed under a compressive load of 1 kPa. This shift is slowly reversible, with the original state and color of the film being recovered a few minutes after release of the pressure. This pressure-sensitive material works in the 0 to 1000 Pa pressure range.[88,89] Despite being better than the first film, its mechanical stability and recovery time are not perfect. Modification of the PEGMA gel with 2-methoxyethyl acrylate yielded a water-free, robust, and fast-responding composite that was tested with a piezoelectric modulator. The total range of the wavelength shift is 172 nm and is sensitive to modulation frequencies up to 200 Hz.[90] This material is deemed to be extremely useful.

6.2. Thermoresponsive Photonic Crystals

Such materials can be used in place of conventional optical probes and sensors for temperature.[91] Two types of thermally responsive PhCs are typically found in the literature, namely those based on polymer swelling, and those based on phase transitions when incorporated into inorganic host materials. The outstanding studies by Asher and co-workers[92] resulted in several combinations of polymer/PhC materials that typically consist of colloidal crystals embedded in a thermosensitive hydrogel, such as poly(*N*-isopropylacrylamide) (PNIPAM), which has a low critical solution temperature (32 °C). PNIPAM expels water from the voids in the polymer at this temperature, and this leads to shrinkage. The change in volume is fully reversible between 10 °C and 35 °C, and the reflected wavelength can be adjusted over the whole visible range. Colloidal crystals without a host matrix (i.e. consisting of pure hydrogel nanoparticles) displayed a small wavelength shift of about 5 nm only. However, the intensity of reflected light decreases as the temperature increases.[92,93] Modification of the PNIPAM colloids made from 2-hydroxyethyl acrylate and divinylsulfone improved the thermal stability and response time.[94] It was also demonstrated that a PNIPAM colloidal crystal array can undergo diffraction shifts even on a nanosecond time scale.[95]

Alternatively, PNIPAM and poly(*p*-methylstyrene) can be used to produce 1D PhCs that change the wavelength of their reflection band with temperature.[96] New strategies include a) the synthesis of thermoresponsive soft core/shell microspheres by using microfluidic techniques,[97] and b) the combination of a poly(methyl methacrylate) (PMMA)

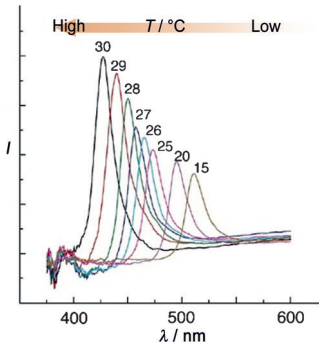

Figure 5. Thermoresponse of the reflectance of interconnected PNIPAM nanoparticles. The color changes from blue to green on going from 30 to 15 °C. Figure adapted from Ref. [101] with permission; copyright 2006 American Chemical Society.

inverse opal with liquid crystals.[98] The use of close-packed silica particles as a template is another approach[99–101] that can be combined with the use of PNIPAM.[102] The spectral changes of a typical thermoresponsive PhC in the visible range are shown in Figure 5.

Hybrid particles that respond to two parameters have also been reported. For example, copolymerization of *N*-isopropylacrylamide and methacrylic acid leads to a gel that is sensitive to a temperature range of 15 to 40 °C and acidity at pH values between 2 and 7. The sensitivity to pH changes leads to a wavelength shift of around 150 nm, while temperature only induces a shift of 50 nm at pH 7 and of 20 nm at pH 2. This is the first approach to PhCs with dual sensitivity, but improvement of the signal range, selectivity, and sensitivity is still ongoing.[103]

Thermally responsive PhCs based on phase transitions in inorganic material hosts have advantages over the use of hydrogel hosts, for example, better thermal stability and faster response time.[21] The distance between particles (and the refractive index) will change during the course of a phase transition, and this will lead to a measureable variation in the intensity of reflected light. Core–shell particles consisting of a selenium core and an Ag_2Se shell undergo a temperature-dependent change in light reflection (of around 130 nm) on going from 70 to 140 °C. This enables measurements above the boiling point of water.[104] Materials such as $BaTiO_3$, VO_2, and silicon can also be used[105–107] for the preparation of thermally sensitive PhCs. The combination of a thermoresponsive Bragg stack PhC with the technology of organic light-emitting diodes (OLEDs) even allows for a color readout by conventional cameras.[108]

6.3. Optically Responsive Photonic Crystals

Irradiation with UV/Vis light can induce changes in the distance of the lattice and of the refractive index of a PhC. This was used to design optically responsive PhCs. In a typical example, the surface charge of silica nanospheres coated with Malachite Green carbinol base is altered on UV irradiation. The resulting change in Coulomb interaction leads to an order/disorder phase transition and to altered optical properties.[77] A polymer/crystal composite containing a covalently bonded azobenzene or spirobenzopyran chromophore changes its volume as a result of photoisomerization of the molecules after irradiation with UV/Vis light. Isomerization causes a volume change in the polymer matrix, and this results in a shift in the reflected wavelength. The process is reversible, but slow (on the order of minutes).[109,110] Another approach to optically responsive PhCs is based on liquid crystals.[78,79] The nematic/isotropic phase transition of the photochromic liquid crystals 4-butyl-4′-methoxyazobenzene and 4-pentyl-4′-cyanobiphenyl form the basis of a switchable light-sensitive PhC if incorporated into an inverse silica opal.

6.4. Electrically Responsive Photonic Crystals

There are two types of electrically responsive PhCs: those that can be stimulated by an external electrical signal,[111] and those that respond to an electrochemical stimulus. The first type is mainly based on a combination of PhCs with liquid crystals (LCs). A change in the orientation of an LC in an applied electric field causes a change in the refractive index which results in a shift of the reflected wavelength. The inclusion of a nematic LC in a silica opal yields a composite whose wavelength shifts by 5.5 nm if a voltage of 160 V is applied.[112] The larger inclusion capability of an inverse opal structure leads to a better tuning ability and a larger wavelength shift (35 nm), but only at higher voltages, typically 300 V.[113]

The second type (which is more important from a chemical viewpoint) generally requires a redox-active compound such as polyferrocenylsilane to become responsive to an electrochemical stimulus. A typical composite consists of a silica colloidal crystal array on an indium tin oxide (ITO) coated microscope glass slide. This array is soaked with a low-molecular-weight polyferrocenylsilane with polymerizable groups (such as an olefin group) and a photoinitiator. After photopolymerization, this composite is fixed in position by a second ITO-coated glass slide. If an oxidation potential is applied to this sensor layer, swelling of the polymer occurs and results in a shift of the reflected light to a longer wavelength. In contrast, a reduction potential allows the composite to shrink and this induces a shift to a shorter wavelength.[114,115] Again, the choice of an inverse opal structure instead of an opal structure improves the performance. In this material, a small bias of 2.8 V causes a shift as large as 300 nm.[116] Other approaches are based on polyelectrolyte hydrogels. Examples of electrochemically responsive PhCs include copolymers prepared from *N*-isopropylacrylamide and methacrylic acid,[117] from 2-hydroxyethyl methacrylate and 3-(methacryloylamino)propyltrimethylammonium hexafluorophosphate,[118] or from styrene and 2-vinylpyridine in a 1D PhC.[111]

6.5. Magnetically Responsive Photonic Crystals

Magnetically responsive PhCs are a special case, in that a magnetic species typically must be included directly in the

colloidal spheres in order to respond to an external stimulus without further modification.[119–121] The incorporation of Fe_3O_4 (magnetite) nanoparticles into monodisperse, highly charged polystyrene nanoparticles yielded a PhC where the wavelength of the reflected light could be adjusted by application of a magnetic field. However, the properties of the composite, such as signal range and response time, require further research. Currently, the application of a 0.24 Tesla magnetic field causes a maximum wavelength change of only 10 nm and requires 60 minutes until equilibration is accomplished.[122,123] Another approach[124,125] is based on the synthesis of 30–180 nm sized colloidal nanoclusters based on magnetite. The resulting PhCs can be fully reversibly tuned from the blue (450 nm at an applied magnetic field of 0.0352 Tesla) to red region (730 nm; at 8.78×10^{-3} Tesla), as can be seen in Figure 6. This is achieved by increasing the distance between the magnet and the vial containing such PhCs from 2.0 to 3.7 cm (Figure 6). To achieve periodic arrangement in solvents other than water, the nanocrystals are typically covered with a silica shell to form more stable dispersions.[126–128]

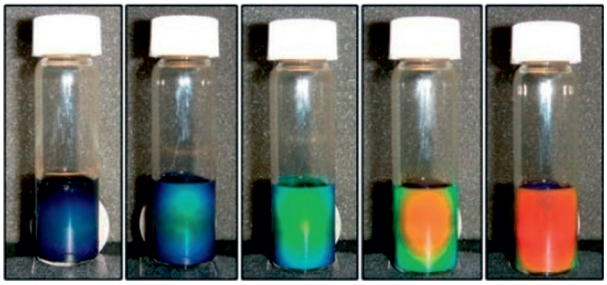

Figure 6. Change in color of colloidal magnetite nanocrystal clusters with decreasing magnetic field strength (from left to right). Adapted from Ref. [125] with permission; copyright 2007 Wiley-VCH GmbH.

The methods based on materials that can be magnetically tuned make use of the distance dependence of particles in a PhC. Alternatively, a change in the orientation may be exploited to alter the reflected wavelength. In one example, colloidal $CoFe_2O_4$/polystyrene nanoparticles in a polyacrylamide host were ground to small pieces and then dispersed in water. In the absence of a magnetic field, reflectance is weak. The application of a field parallel to the detection unit results in the light reflectance being strongly increased because of the particles becoming more ordered. If the orientation is disturbed again by applying a second field in the vertical direction, the effect is reversed.[129]

7. Photonic Crystals Responsive to Solvents, Vapors, and Chemical Species

There are numerous situations where chemical sensors are needed that are small, portable, easy to handle, and capable of on-line monitoring a chemical species, ideally with a visual (naked-eye) readout. Sensors based on the use of PhCs are promising candidates in this respect,[130] not the least because they are not affected by electromagnetic fields. One may discern between chemically responsive PhCs based on porous structures with a tunable refractive index, and those based on the shrinking and swelling of polymers. The first are the materials of choice for distinguishing solvents through differences in the refractive index (RI). Inverse opal materials, that is, materials with a 3D periodic hole structure such as oxides of silicon, aluminum, and zirconium, give a significant response to the application of different solvents.[131–134] Mesoporous (1D) Bragg stacks consisting of various inorganic materials can differentiate organic solvents particularly well.[71,72,135–137] Table 1 shows that such PhC-based sensors are able to detect changes with a resolution of 0.001 RI units per nm. Sensors based on surface plasmon resonance have a resolution that is a factor of at least 500 better, but require a more complex instrumental readout.[138]

Table 1: Sensitivity of mesoporous Bragg stacks to refractive index (RI) as a function of the number of layers.

Material	Number of layers	RI	λ [nm]	Resolution[a]	Ref.
SiO_2/TiO_2	2-6	1.36–1.42	545–575	0.002	[136]
SiO_2/TiO_2	6	1.33–1.53	500–700	0.001	[72]
Si/SiO_2	20	1.33–1.53	1560–1620	0.003	[137]

[a] Resolution in RI units per nm.

The degree of compound uptake has to be closely controlled to achieve chemical selectivity when sensing changes in the refractive index. The small pore sizes in mesoporous materials allow for selective surface adsorption to have a significant impact on the total uptake of material, as shown in the study by Bonifacio et al.[71] on a PhC-based chemical nose. A similar device makes use of the selective wetting of inverse opals by tuning the bulk filling of the porous material[133,134] to achieve better specificity than that achieved, for example, by the research groups of Ozin or Míguez.[72,135,136,139] The method was further refined[140] by combining mesoporous photonic crystal beads that had been modified with 16 different alkoxysilanes. This led to an array that functioned as an optical nose chip for the detection of organic vapors. Figure 7a shows a digital image of the respective 16-spot chip (array), and Figure 7b the reflection spectra of the bead in the spot.

The same assembly was used to measure the vapor pressure of 2-propanol.[139] The exchange of SiO_2 in the layer structure by a mixed-metal oxide led to a sensor for volatile organic compounds (VOCs).[141] A sensor for VOCs was also obtained by combining a porous silicon PhC with an optical fiber waveguide[142–144] and with an LED.[145] A stack of three mesoporous silicon-based PhCs was shown[146] to enable time-resolved identification and quantification of VOCs at ppm levels. Another kind of sensor (with naked-eye readout) was constructed by depositing a gradient of long-chained alkylsilanes with different head groups (methyl, carboxy, hydroxy) on porous silicon. It allows for the determination of ethanol in

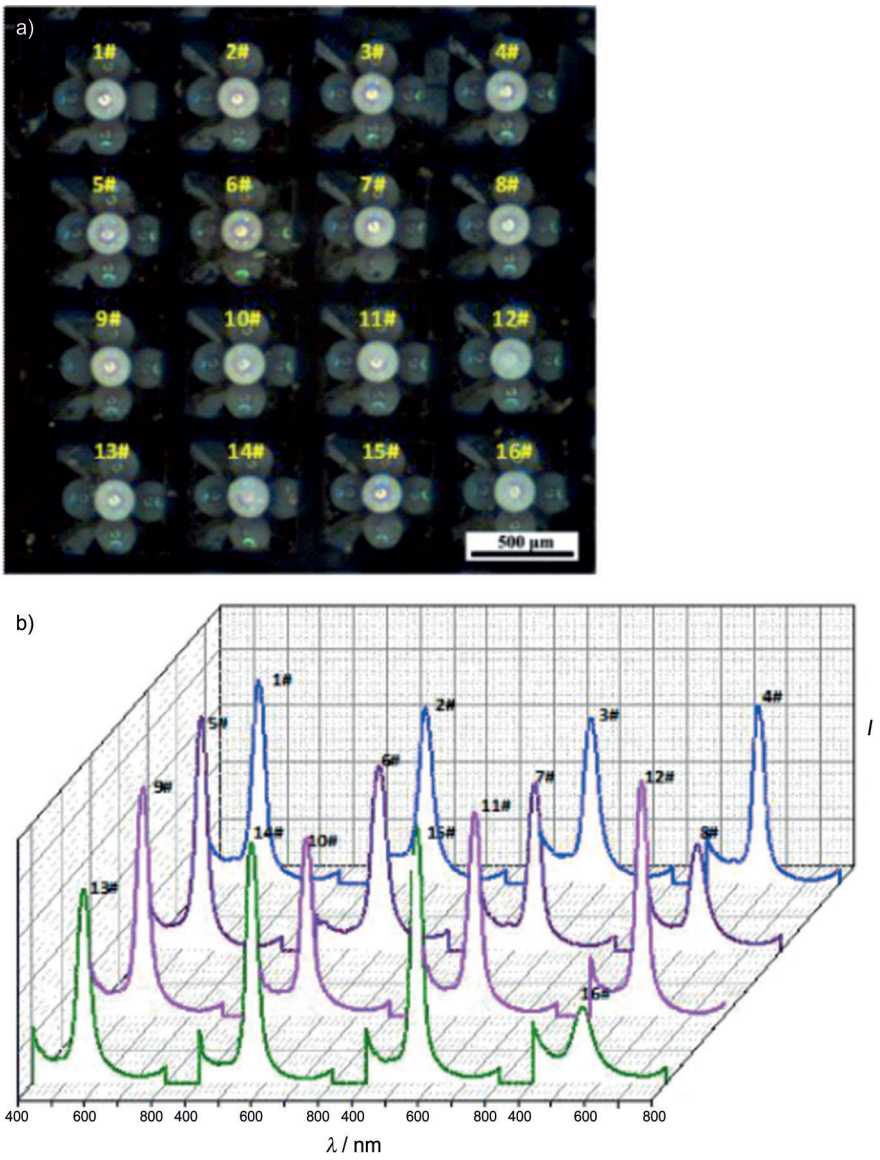

Figure 7. a) Digital image of a 4×4 photonic crystal sensor array. b) Reflection spectra of the beads in the 4×4 array. Adapted from Ref. [140] with permission; copyright 2014 Wiley-VCH GmbH.

water at concentrations between 0 and 8% with a resolution of 1%.[147] The combination of a microporous metal–organic framework (known as ZIF-8) with layers of mesoporous titanium dioxide was used[148] for discriminating between methanol, ethanol, 2-methylbutanol, and *tert*-pentanol. A two-dimensional TiO_2 pillar array can differentiate fluids with a refractive index in the range between 1.33 and 1.39 with a resolution of about 0.002 RI units per nm.[149] A zinc sulfide nanobowl array[150] was assembled from polystyrene nanoparticles as well as zinc and sulfide precursors and enabled the refractive index of organic solvents to be determined over an even wider range (from 1.33 to 1.50) but at lower resolution (ca. 0.004 RI units per nm).

Another solvent-selective PhC sensor that, in fact, detects changes in refractive index was obtained[151] from butterfly scales of the *Morpho* species (see Section 2). This approach has certain limitations though, in that it depends on the use of matter produced by living creatures and thus issues of reproducibility and large-scale production require particular attention. One-dimensional PhC sensors made from mesoporous silicon have also been designed to determine relative humidity,[152–154] gaseous ammonia and gaseous chlorine,[155] and gaseous hydrofluoric acid.[155] However, complex mixtures of fluids and mixed gaseous samples have not been investigated so far.

A simple 1D periodic lamellar structure was fabricated in the form of alternating layers of hydrophilic and hydrophobic block polymers (Figure 8). In essence, this is a type of a Bragg stack with layers of two different polymers. The hydrophobic and more rigid layers force expansion of the hydrophilic copolymerized layers into the *z*-direction (i.e. vertically), while expansion into the *x*- and *y*-directions is prevented by the hydrophobic copolymer. The resulting PhC responds by a swelling of the hydrophilic layers. This was successfully demonstrated by exposing the sensor layer to a 75 mM solution of ammonium chloride.[156] The selectivity for chemical species will clearly be limited.

The second type of chemoresponsive PhCs (based predominately on 3D swelling and shrinking) forms the basis for numerous other sensors. Again, organic solvents may be detected that cause such effects (Table 2),[80–82,157–160] but selectivity remains poor because such gels respond only to polarity, and not specifically to a certain solvent. If the correct materials are used, the sensors will also respond predictably to vapors of organic species.

Organic solvents may also be detected and determined solely by PhCs with an opal structure[161] or an inverse opal structure[162–165] without the need for a hydrogel matrix. The inverse structures are obtained by permeating a 3D opal with sol–gel precursors, such as those for making SiO_2,[162,164] or ceria.[163] After completion of the inverse opal shell, the template is removed. A related approach is based on the use of a metal–organic framework[165] to build a solvent-sensitive inverse opal PhC. Conceivably, such a material will be unstable in certain organic liquids, but the inorganic oxides (which, unfortunately, hardly respond to organic solvents) may be replaced by more-responsive metal–organic materials.

Takeoka and co-workers used the phase separation of a self-assembled polymethacrylate ester to detect solvent impurities in toluene.[166] The wavelength of the transmitted

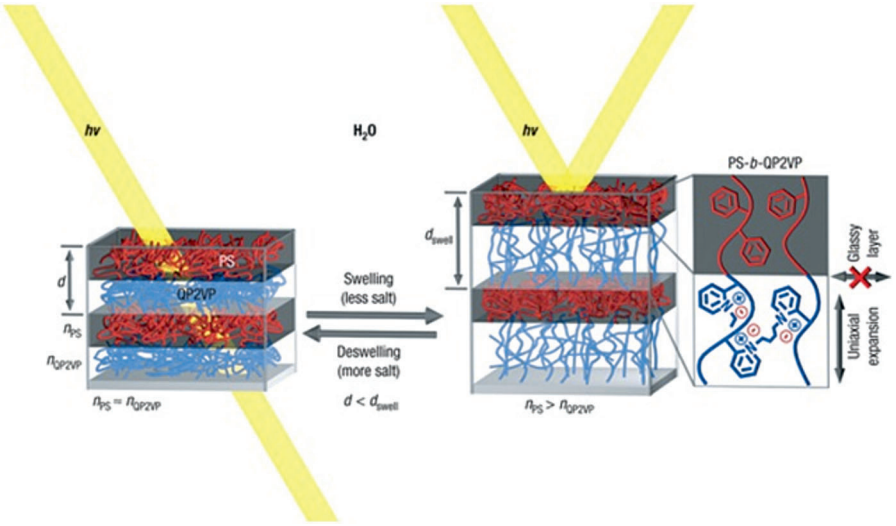

Figure 8. Schematic representation of a photonic gel film prepared by the self-assembly of layers of hydrophobic and hydrophilic copolymers. Swelling and shrinking of the hydrophilic gel layers (blue) by aqueous solvents modulates both the domain spacing and the refractive-index contrast, and accordingly shifts the wavelengths of the reflected light (*hν*). The hydrophobic and glassy polystyrene layers (red) limit the expansion of the gel layers in the direction perpendicular to the layers. Reprinted from Ref. [156] with permission; copyright 2007 Macmillan Publishers Ltd.

light changed from 400 to 700 nm between 83 and 100% toluene. The swell/shrink process was also exploited in a sensor for relative humidity.[167–170] Another approach utilizes the different molecular conformations that PNIPAM adopts in different hydration states.[171] The fabrication of an inverse opal consisting of carbon resulted in an oil-sensitive PhC sensor that responded to refractive indices between 1.37 and 1.66.[172]

Various PhC-based sensors have been reported that enable the determination of pH values and of ionic strength.[74,76,83,173–176] In a typical process to fabricate such a sensor film, nanoparticles are incorporated into a polyacrylamide hydrogel matrix. The resulting layer exhibits a reversible wavelength shift of around 250 nm on going from pH 2 to pH 7. However, the method described for the readout is rather complex. Typical materials and properties of pH sensors are summarized in Table 3.

Ionic strength (IS) plays an important role in physiology and also determines the salinity of seawater. The first method for sensing pH and IS was introduced by Lee and Asher.[74] However, they only tested solutions of sodium chloride in the range of 0 to 10 mM. Zhang et al. carried out a similar study with PNIPAM microgel crystals, but with NaCl concentrations of up to 750 mM.[177] In a detailed study, Fenzl et al.[83] showed that such sensors responded to the IS of various electrolyte solutions and gave an almost linear response to the log value of the salt concentration in the range from 50 μM to 10 mM (Table 3).

The ethanol-assisted self-assembly of polystyrene spheres and their incorporation into a poly(vinyl alcohol) hydrogel results in a PhC that is responsive to a) various solvents, b) various cations and the pH value, and c) compressive strain.[178] Such sensors are of limited practical utility due to their poor selectivity. More specific and ion-selective PhC-based sensors have even been reported.[179,180] Selectivity for potassium was accomplished, for example, by the introduction of crown ethers (that can bind alkaline and other ions fairly selectively) into the hydrogel. An increase in the potassium ion concentrations from 0 to 40 mM cause a spectral shift of 200 nm in the wavelength of the maximum diffraction.[181] A sensor for lead(II) ions also utilizes crown ethers as molecular receptors. The shift in wavelength is about 150 nm at lead(II) concentrations between 0 and 10 mM.[182–186] In another method for sensing metal ions, a PhC based on poly(vinyl alcohol) (PVA) was modified with the optical indicator 8-hydroxyquinoline to (unselectively) respond to copper, nickel, and zinc cations,[187] possibly also to magnesium. Anions, in turn, can be selectively detected either with a photonic ionic-liquid polymer[188] or by hydrogel opal structures with a water-tunable photonic band gap.[189] A 2D array of polystyrene particles placed in a poly(*N*-isopropylacrylamide) matrix was found to be responsive to ionic surfactants such as sodium dodecyl sulfate (anionic) and cetyl trimethylammonium bromide (cationic).[190]

PhC-based chemical sensing was also combined with the molecular imprinting (MIP) technique. In this approach, an array of colloidal spheres—mostly silica or polystyrene—is soaked with a mixture of polymerizable monomers, a polymerization initiator, and the analyte. After polymerization, the template is removed to create voids into which the analyte from a sample may diffuse if it fits. MIP-based sensing with PhCs has been described for BSA, egg albumin, and lysozymes,[191] where silica spheres were used as the template and a copolymer made from methacrylic acid and ethylene glycol dimethylacrylate (EGDMA) was imprinted with the desired analyte. Concentrations as low as 1 $\mu g L^{-1}$ caused a detectable shift in the reflected wavelength.

Bisphenol A (BPA) was quantified[192] with a resolution (expressed in terms of concentration per wavelength shift) of 0.014 $\mu M\,nm^{-1}$ by using the materials described above.[191] In another approach, BPA was imprinted directly into the PMMA spheres, and these were then placed on a glass substrate by a vertical deposition technique. This led to a sensor that can detect 1 $\mu g L^{-1}$ of bisphenol A with a clearly detectable red-shift of the reflected light.[193] Cholesterol was imprinted into a copolymer prepared from acrylic acid and methacrylic acid and allowed its detection at levels as low as 1 $ng L^{-1}$. The selectivity is surprisingly good; stigmasterol and ergosterin, for example, do not cause a wavelength shift.[194] Similarly, vanillin was imprinted[195] into a cross-linked PMMA inverse opal structure which resulted in a sensor that can detect vanillin in concentrations down to 1 pM. Yuan

Table 2: Overview of materials used in photonic crystal (reversible) sensors for organic solvents, the respective wavelengths of maximal reflection (on air; in nm), and the spectral shift cause by solvent or vapor (in nm).[a]

Material	Reflected wavelength	Wavelength shift for respective solvent														Ref.
		methanol	ethanol	*n*-propanol	2-propanol	hexanol	acetone	acetonitrile	THF	DMF	DMSO	silicone oil 0.65 cSt.	silicone oil 20 cSt.	silicone oil 50 cSt.	hexane	benzene	toluene	xylene	
PS/PDMS	420	5	20									137			151				[82]
PS/PDMS	450											135	35						[80]
PS/PDMS	550											150		20					[81]
PS/PDMS	440		90		100	85									250				[81]
PS/PDMS	550	< 10	< 10				140									360	400	420	[157]
PS/polyacrylamide	610	−150	−150	−150															[158]
PMMA-*co*-PHEMA-*co*-PEGDMA/TiO_2	340		62					113		253	388	420							[159]
silicon/polystyrene	705		40																[160]

[a] PDMS = polydimethylsiloxane, PHEMA = poly(2-hydroxyethyl methacrylate), PS = polystyrene.

et al.[196] used polystyrene opals and a polyacrylamide hydrogel for imprinting 3-pyridinecarboxamide and were able to detect a 1% aqueous analyte solution with a shift of 27 nm relative to a negative control, as the imprinted hydrogel changes its reflected wavelength as a result in a change in the volume of the hydrogel film in the presence of the analyte. Such sensors display limited selectivity because the hydrogel itself is sensitive to matrix effects, for example, as a result of a change in the pH value. Chiral recognition of L-pyroglutamic acid in concentrations between 0.01 and 0.5 mM was achieved by imprinting the amino acid into a polystyrene PhC.[197]

The Berthelot reaction (based on the reaction of an alkaline solution of phenol and hypochlorite with ammonia to form a blue indophenol) was used[198] in a 3D PhC to determine ammonia. The photonic effect is caused by the indophenol generated, which induces new cross-links in the hydrogel. This, in turn, results in a blue-shift of the reflected wavelength. A TiO_2 inverse opal was soaked with aniline and potassium peroxydisulfate and then polymerized to form a responsive layer.[199] It was reported to reversibly change its reflective color in the presence of ammonia or hydrochloric acid as a result of acid–base reactions in the polymer causing changes in the refractive index of the polymer layer which resulted in a wavelength shift of the reflected light.

Glucose (like many other saccharides) undergoes a fully reversibly binding reaction with certain boronic acids, and this can be used for quantitative assays.[200] The respective PhC sensor was obtained from polystyrene spheres and a polyacrylamide hydrogel functionalized with 3-aminophenylboronic acid. This material responds to glucose in concentrations of up to 100 mM, however with a signal change of only a few nanometers at 4 mM (which is the typical concentration of glucose in blood). Signal changes also occur with fructose, galactose, and mannose, but these are usually present in much lower concentrations in blood. Similarly, a crystalline colloidal array (CCA) was incorporated into a polyacrylamide hydrogel (PCCA) with pendent boronic acid groups, as shown schematically in Figure 9. The CCA diffracts visible light, and the PCCA diffraction wavelength is dependent on the hydrogel volume. The PCCA responds to carbohydrates, in particular to aqueous solutions of glucose with a low ionic strength, by swelling and red-shifting its diffraction. The hydrogel swelling results from a Donnan potential as a result of the formation of the boronate anion whose acid pK_a value decreases upon glucose binding. The sensor was incorporated into a contact lens to visually monitor glucose concentrations in tear fluid.[75,201–203] In yet another version of a glucose

Figure 9. Incorporation of a phenylboronic acid (acting as a receptor for glucose) into a 3D PhC. GL: glucose. Reprinted from Ref. [75] with permission; copyright 2004 American Chemical Society.

Table 3: pH-Sensitive photonic crystals, respective analytical wavelengths, pH ranges, and effects of ionic strength.

Material	λ [nm]	pH	Linear pH range	Ionic strength range [M]	Ref.
polystyrene/polyacrylamide	430–550	1–9	3.5–4.5	10^{-6}–6×10^{-1}	[83]
polystyrene/quaternized poly-(2-vinyl pyridine)	450–600	2–7	–	–	[173]
polystyrene/poly(acrylamide-*co*-acrylic acid)	620–670	2–8	3.5–4.5	–	[174]
SiO_2/poly(hydroxyethyl methacrylate-*co*-methacrylic acid)	520–640	3.5–9	5–6	–	[76]
polystyrene/polyacrylamide	500–800	2–9	–	10^{-4}–10^{-2}	[74]
polystyrene/poly(vinyl alcohol)/succinic acid	445–485	2.5–6	3.5-4	–	[175]
polystyrene/poly(vinyl alcohol)/3-aminophenol	410–450	7–10.5	9.5-10	–	[175]
morpho butterfly wing scales/polymethylacrylic acid	466–492	1.5–10.5	–	–	[176]

sensor,[204] the block copolymer polystyrene-*co*-poly(2-vinyl pyridine) was modified with 2-(bromomethyl)phenylboronic acid to give a material capable of selectively detecting fructose even in the presence of glucose, mannose, and sucrose. The limits of detection are 500 μM of fructose in plain water and 1 mM in phosphate-buffered saline, which indicates an effect of the ionic strength.

8. Biosensors Based on Photonic Crystals

Biosensors make use of biological components such as enzymes, antibodies, aptamers, and gene probes to recognize a specific target. Typical applications of such sensors[205] are in the screening of compound libraries and of ligand–receptor interactions (such as between biotin and streptavidin), in label-free optical detection, and in studies on cell morphology. Creatinine is a clinically highly relevant parameter that can be sensed with PhCs by using the enzyme creatinine deiminase. The effect is due to the swelling of hydrogels as a result of two consecutive reactions: First, creatinine deiminase causes the production of hydroxide ions by hydrolysis of creatinine. In a second step, 2-nitrophenol (also incorporated in the hydrogel) is deprotonated by the hydroxy ions formed. The increased solubility of the phenolate anion causes the swelling in the polymer (Figure 10). The red-shift in the diffraction is approximately 35 nm at 1 mM levels of creatinine. The change is, however, much smaller (15 nm) at typical physiological concentrations (100 μM).[206]

Cholesterol was also detected enzymatically in concentrations of up to 5 mM by linking cholesterol oxidase (ChOx) to an epoxide-functionalized hydrogel-based PhC prepared from acrylamide and glycidyl methacrylate[207] and was referred to as a polymerized crystalline colloidal array (PCCA). The bound enzyme retained about 85 % of its initial activity. Upon exposure to 5.0 mM cholesterol, the maximum diffraction wavelength was red-shifted by as much as 63 nm compared to the negative control. Detection is again based on hydrogel swelling: Changes in the Donnan potential of ChOx causes swelling of the polymer and, therefore, a shift of the reflection signal.

Organophosphate nerve agents can be detected and quantified by making use of the enzymes acetylcholinesterase and organophosphorus hydrolase in modified PhCs.[208,209] Both sensors utilize the fact that the hydrogel host shrinks or swells as a result of changes in the polarity of the

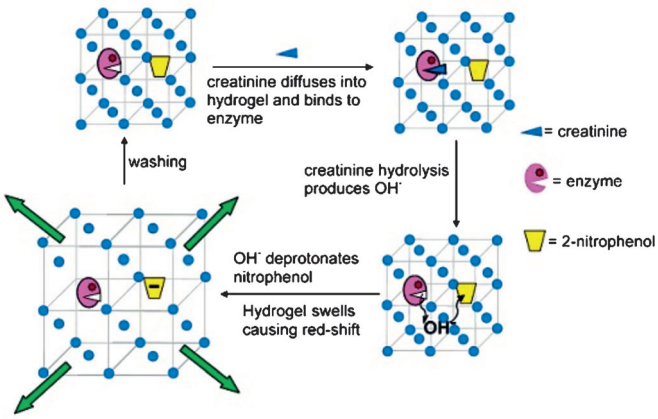

Figure 10. Schematic depiction of the creatinine sensor concept. Creatinine deiminase causes the production of hydroxide ions. In a second step, 2-nitrophenol is deprotonated. The increased solubility of the phenolate ion and its negative charge causes the swelling in the polymer. Adapted from Ref. [206] with permission; copyright 2004 American Chemical Society.

environment. Acetylcholinesterase is capable of binding parathion, and this causes swelling and a red-shift of the maximum of the reflected light.[208] Organophosphorus hydrolase, on the other hand, produces two protons on hydrolyzing parathion, and this causes the polymer to shrink, which results in a blue-shift.[209] Mercury is a strong inhibitor of the enzyme urease. By analogy to a known fluorescent detection scheme based on this effect,[210] a Hg^{II}-selective PhC sensor probe was described.[211] The hydrolysis of 1 mM urea caused by urease results in a blue-shift in the reflected wavelength from 764 to 646 nm because of the increasing ionic strength of the medium as a consequence of the generation of both ammonium and bicarbonate ions. If the enzyme is inhibited by Hg^{II} ions, a shift from 646 (uninhibited hydrolysis) to 730 nm is obtained on increasing the concentration of the inhibitor from 0 to 20 ppb. However, other heavy metal ions are also likely to cause an effect. A poly(acrylamide-*co*-acrylic acid)-based PhC hydrogel that was modified with a tetracycline-copper(II) complex was shown[212] to respond to the model amino acid glycine at a concentration as low as 100 pM. Here, the diffraction band is even located in the near infrared region.

PhC sensor technology was also used to detect ligand–receptor interactions. A silicate layer that forms the top of an SiO_2/Ta_2O_5 Bragg stack was modified[61] with streptavidin (each molecule of which can bind four biotin molecules). On

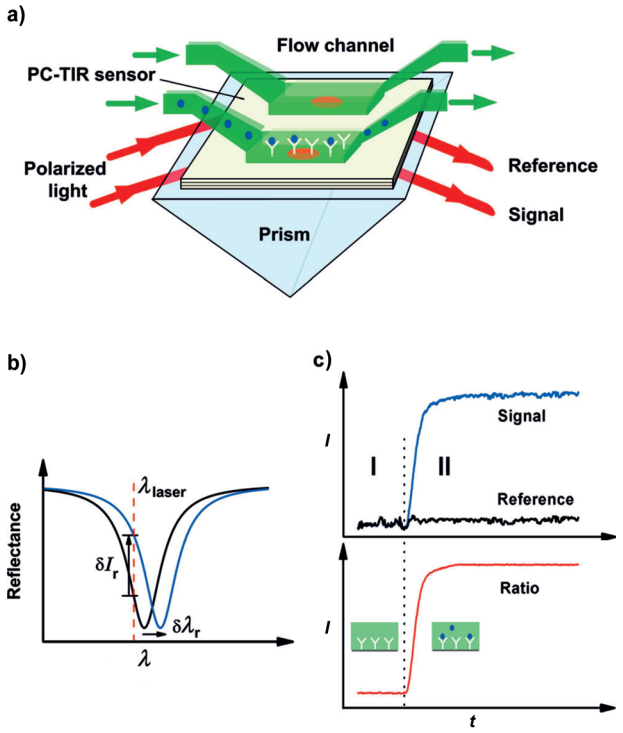

Figure 11. Fabry–Pérot resonator based on a 1D PhC coupled with total internal reflection (TIR). a) Schematic sensor configuration on separate signal and reference channels. b) The resonance mode shift ($\delta\lambda_r$) can be monitored by directly observing the reflectance spectrum or by measuring the reflected intensity change (δI_r) at a specific laser wavelength. c) Binding kinetics monitored by the reflected signal intensity and by the normalized intensity ratio, where region I is the baseline with ligand on the surface and region II reflects real-time analyte binding to ligand. Adapted from Ref. [213] with permission; copyright 2010 American Chemical Society.

binding biotin, the refractive index of the top layer changes, and this results in a wavelength shift of the reflected light. The resulting signal change was detected with a Fabry–Pérot resonator incorporating a prism coupler and a Bragg reflector (Figure 11). Biotin can be monitored by this method with a limit of detection (LOD) of 3 $\mu g\,mL^{-1}$. The same principle was applied to follow the binding of a wide range of other biomolecules by their respective receptors[213,214] with molecular masses ranging from 0.244 to 150 kDa. The detection of a biotinylated 20-base oligomer had an LOD of 1 nM. Guo et al. emphasized[213] that this approach results in a more easily detectable resonance signal than that obtained by total internal reflection spectroscopy. In this detection approach for oligomers, an energy-loss mechanism is triggered in the dielectric stack in that light is absorbed in the silicium layer which generates defects in the top dielectric. This allows light (that would otherwise be resonant in the dielectric cavity) to penetrate the analyte solution.

PhCs also can be modified with nucleotide oligomers (including aptamers) such that gene sensors are obtained. Particles consisting of a styrene, methyl methacrylate, and acrylic acid copolymer were used[215] for sensing DNA at 13.5 fM levels. The PhC was used here to enhance the fluorescence of a FRET-based DNA detection approach

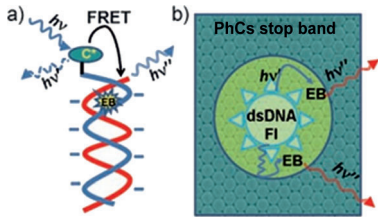

Figure 12. a) DNA sequence detection based on a FRET mechanism. After hybridization, ethidium bromide (EB) can intercalate and forms a FRET couple with fluorescein-labeled ssDNA. b) Effect of the PhC on the efficiency of FRET. The periodicity of the PhC amplifies the fluorescent signal and improves the limit of detection. Adapted from Ref. [215] with permission; copyright 2008 Wiley-VCH GmbH.

(Figure 12). The functionalization of silica colloidal arrays with DNA led to a PhC sensor with the ability to detect bacterial pathogens[216] or hybridization/denaturation processes.[217] The metal ions Pb^{II} and Hg^{II} were detected with an irreversible PhC-based optical probe that is based on the functionalization of the PhC hydrogel matrix with aptamers.[218] This approach is entirely different from the enzyme-based detection method for heavy metal ions described above. The short nucleotide strands were immobilized in a hydrogel and change their conformation in the presence of the heavy metal ion they were designed for. This causes a volume change of the polymer and a blue-shift of the diffraction band.

Immunoassays based on PhCs include a multiplexed immunoassay[65] based on a nanoscale optofluidic system and an array of evanescently coupled 1D PhC resonators. The device enabled antibodies against interleukin to be determined in the 1 to 100 $\mu g\,mL^{-1}$ concentration range and with an LOD as low as 0.06 fg(!) of totally bound mass. A similar kind of biosensor (a 2D silicon-on-insulator PhC sensor)[219] can detect 2.5 fg of bovine serum albumin.

The binding of BSA (and probably also of other proteins) to glutaraldehyde in the microcavities of the porous silicon sensor causes a red-shift of the reflected wavelength. As the interaction of glutaraldehyde and BSA is nonspecific, the authors also tested the device with immobilized streptavidin and found a biotin-specific red-shift in the reflected wavelength. This device works at a wavelength of around 1.5 μm, which was chosen (such as the integrated design) to obtain a platform that is CMOS-compatible and can be integrated on a large scale (e.g. in consumer electronics). Both sensors[203,204] have the advantage of possessing very high so-called Q factors so that the electromagnetic energy can be localized very accurately, and they display narrow bandwidth spectra that enable the precise determination of the wavelength of the resonance peak. Both factors contribute to the fact that very small quantities of bound mass can be detected. In another immunodetection approach, protein A was deposited on a porous silicon PhC by nonspecific adsorption. Three kinds of immunoglobulins were then detected[220] because they bind to protein A. Human, sheep, and chicken IgG were distinguished because their refractive indices are different. Binding (and thus the optical effect) is irreversible.

Microplates with nanowells incorporating PhCs were prepared[221] by electron beam nanolithography and combined

with an electrophoretic particle entrapment system. These immuno platforms were used for detection of the food-borne staphylococcal enterotoxin B (SEB). Polystyrene nanoparticles were modified with anti-SEB antibody and entrapped in the nanowells. Upon binding of the SEBs and after addition of a fluorescently labeled anti-SEB secondary antibody, the signal corresponding to a guided mode resonance is amplified by the PhC structure. SEB can be determined at levels as low as 35 aM, an LOD that is 106-fold better than that of a conventional 96-well ELISA. The method was applied to milk samples (known to be a rather difficult matrix), where the LOD was not significantly altered. A related immunoassay[222] is based on the use of a 2D silicon PhC and enables the detection of anti-BSA binding to surface-immobilized BSA.

The Endo research group[223] showed that the fluorescence intensity of DNA intercalators can be strongly enhanced by using nano-imprinted 2D PhCs. Highly ordered 2D PhCs prepared from a cycloolefin and possessing triangle-shaped and nanometer-sized hole arrays were deposited on a 100 μm thick polymer film by nanoimprint lithography. Double-stranded DNAs (in lengths of 4361 and 48502 base pairings and in concentrations from 1 pM to 10 nM) were adsorbed on the surface by electrostatic interactions and then treated with intercalators. The fluorescence of the intercalator was found to be enhanced by factors of up to 10 (compared to the usual enhancement by intercalators). If the PhC is used as a Bragg reflection mirror, the fluorescence enhancement can be easily observed visually or using a spectrofluorometer. These results suggest that printed PhCs offer a large potential for sensitive intercalator-based detection of DNAs. A similar 2D PhC sensor (and also based on a polycycloolefin) was modified with anti-insulin antibodies and was then capable[224] of detecting insulin with an LOD of 1 $\mu U\,mL^{-1}$ through a change of the reflection peak intensity upon binding of the analyte. In yet another approach,[225] porous silicon microparticles in buffer solution were functionalized with anti-human CD3 primary antibody. The binding capability of the epitope of the primary antibody was still active after functionalization. The authors consider these findings to represent a first step towards single-cell optical biosensors.

A TiO_2-based inverse opal was modified[226] with IgG through nonspecific adsorption and subsequent BSA blocking. The resulting so-called bioPhC can detect 1 $\mu g\,mL^{-1}$ levels of anti-human IgG. Recently, Gu and co-workers[227] reported on the physical adsorption of IgG on PMMA nanoparticles possessing structural colors. FITC-labeled (FITC = fluorescein isothiocyanate) anti-IgG antibodies bind to these particles, as demonstrated by measuring both the changes in the reflectivity and the intensity of the fluorescence (Figure 13). By encoding different proteins with the structural color of PhCs and using FITC labeled antibodies, Li co-workers[228] demonstrated multiplexed immunodetection of mycotoxins. Aflatoxin B1, fumonisin B1, and citrinin were detected simultaneously with detection limits of 0.5, 1, and 0.8 $pg\,mL^{-1}$, respectively.

The combination of an Si_3N_4/SiO_2 layer array and a 2D PhC enabled[229] the detection of single nanoparticles with diameters of 150 nm or larger, with the particles inside the PhC nanoholes appearing as bright spots in the micrograph acquired with a CCD camera. This proof-of-principle study demonstrated such PhCs to enable the visualization with a conventional optical microscope of particles with a size smaller than the diffraction limit. The authors expect that even biomolecules with a diameter between 50 and 100 nm may be visualized in the future if the SiO_2 component is modified with a biorecognition element.

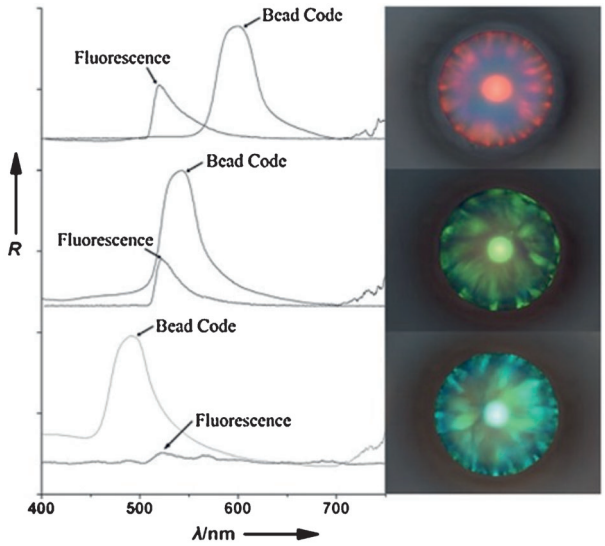

Figure 13. Fluorescence and optical reflection spectra (left) and bright-field microscopy images (right) of three colloidal crystal beads with a diameter of 400 nm. The red, green, and blue beads were modified with human, mouse, and rabbit IgG, respectively. They were exposed to a sample containing FITC-tagged goat anti-human IgG and goat anti-rabbit IgG. Both the fluorescence and reflection measurements were performed. Spectra are offset along the *R* axis for clarity. Adapted from Ref. [227] with permission; copyright 2006 Wiley-VCH GmbH.

In summary, most of these biosensors do not enable a species to be monitored over time.[230] Rather, the performance of hydrogel-based PhCs resembles that of indicators which enable single-shot measurements only, which is more than adequate in many situations for clinical diagnosis. For continuous monitoring, for example of parameters whose concentrations vary over time, it is recommended to choose PhCs based on integrated nanocavities or Bragg stacks.

9. Conclusions and Outlook

9.1 Current and Future Applications

This Review reveals the large scope of PhC-based chemical sensing and biosensing. The question remains as to future applications where such sensors would be superior to existing ones. We believe that low costs (both in terms of materials and production) and the ease of instrumental (if not visible-eye) readout are very strong features of this technique. Mechanically responsive PhCs are an ideal choice for sensors that rely on pressure-dependent color changes. The fingerprint sensor developed by Ozin and Arsenault[231] is a good

example. The use of electrically tunable PhCs in a display is also presented in the same study.[231] Magnetically tunable devices of a similar kind use colloidal PhCs made of magnetite and silica.[127]

Biosensors, in our eyes, have a larger scope than chemical sensors, where the state of the art in sensing conventional parameters (pH values included) is quite advanced. We think that colloidal PhCs that respond to a biochemical stimulus (glucose and other highly competitive clinical parameters not included) hold great promise, in particular for point-of-care parameters for which alternative methods are not available or perform poorly. In our opinion, PhC-based sensing should not aim to replace existing methods but should focus on entirely new fields and parameters. Fast (on-site) testing of food safety is one such area. Methods for the rapid detection of pathogens in food are urgently sought. Pathogen-responsive PhCs, especially if accompanied by a visibly detectable color change comparable to a pregnancy test, potentially have a large market. In fact, respective test stripes may be integrated into the packaging. Semiquantitative tests are adequate in such situations, and small-sized low-cost instrumentation may be used.

PhC-based sensors have also been designed that work (by reflecting light) in the 1–2 μm wavelength range. While not visually detectable, such sensors are compatible with CMOS technology, as shown, for example, by Erickson and coworkers.[65] Such devices are likely to be more sensitive and to offer better resolutions (expressed as the signal change ΔS per concentration unit), for example in high-throughput pharmaceutical screening.[232] In contrast to the widely used colorimetric enzymatic (inhibition) methods that use kinases or proteases and the respective substrates, methods for the detection of protein–protein interactions (in high-throughput screening) often lack the simplicity inherent to enzyme and receptor assays. PhC biosensors (and other emerging technologies) may, therefore, be utilized for the identification of compounds that disrupt or enhance protein–protein interactions. In the medical field, PhC technology is, of course, not limited to the field of chemical sensing and biosensing. Biodegradation processes can be monitored,[233] for example, by implanting an inverse opal PhC consisting of poly(1,5-pentanediol-*co*-pentaerythritol-*co*-citric acid) into subcutaneous tissue of mice. A relatively large shift in the reflection peak is observed due to the deterioration of the PhC through biodegradation.

9.2. Current Challenges

Several challenges are currently limiting the performance of PhC-based sensors. Major issues include selectivity, sensor stability, signal changes, readout schemes, and improved materials. These shall be briefly addressed in the following.

1) *Selectivity* is often not warranted (unless biological recognition is integrated). Many so-called "sensors" are in fact detectors, for example to measure changes in refractive index or solvent polarity, which is useful in numerous situations, but such "sensor detectors" are not selective. Even more specific sensors (such as for pH values of metal ions) are often affected, for example, by the ionic strength of a solution or by other metal ions.
2) Sensor *stability* is compromised in two ways: Storage can lead to (irreversible) changes in the structure (or dimensionality) of PhCs, and this will affect performance and calibration functions. Secondly, some sensors undergo irreversible changes when used, so that recalibration of the sensor becomes mandatory after each single use (which is highly impractical), or sensors are to be disposed of, which is not a problem in terms of costs but is a problem in terms of environmental protection and precalibration of such probes.
3) *Signal changes* need to become larger. *Resolution* (defined as signal change per concentration unit) is often small, so that sophisticated methods for readout become mandatory to accomplish good resolution. Ideally, the change in color is so large that acceptably good resolution becomes possible even by inspection with the naked eye (ideally by making use of a calibration color scale). This would represent a major leap forward and form an attractive alternative to test strips and lateral flow assays.
4) *Readout* schemes (unless visual) need to be simple, but should not be limited to reflectometry, Bragg gratings, or interferometry. Novel schemes with high resolution are sought, for example, by combining it with CMOS techniques and integrated into consumer electronics. Fluorescence also represents an attractive scheme.[215,225–227] Methods for radiative decay engineering (of fluorescence) on one-dimensional photonic crystals have been discussed.[234]
5) *Materials* improvements mainly relate to the homogeneity of the particles (in terms of polydispersity) and an almost perfect crystal structure. Both give rise to high color purity and, thus, to better spectral/color resolution and discrimination. This, eventually, will lead to an alternative generation of test strips of the single-shot probe type and with visual or smartphone-assisted readout, and even to sensors for continuous and on-line monitoring of chemical, biochemical, or biophysical parameters.

Received: September 5, 2013
Published online: January 28, 2014

[1] M. A. C. Stuart, W. T. S. Huck, J. Genzer, M. Müller, C. Ober, M. Stamm, G. B. Sukhorukov, I. Szleifer, V. V. Tsukruk, M. Urban, F. Winnik, S. Zauscher, I. Luzinov, S. Minko, *Nat. Mater.* **2010**, *9*, 101 – 113.
[2] Y. Zhao, Z. Xie, H. Gu, C. Zhu, Z. Gu, *Chem. Soc. Rev.* **2012**, *41*, 3297 – 3317.
[3] P. Vukusic, J. R. Sambles, *Nature* **2003**, *424*, 852 – 855.
[4] A. R. Parker, H. E. Townley, *Nat. Nanotechnol.* **2007**, *2*, 347 – 353.
[5] O. Sato, S. Kubo, Z.-Z. Gu, *Acc. Chem. Res.* **2009**, *42*, 1 – 10.
[6] P. J. Darragh, A. J. Gaskin, B. C. Terrell, J. V. Sanders, *Nature* **1966**, *209*, 13 – 16.
[7] X. Gao, X. Yan, X. Yao, L. Xu, K. Zhang, J. Zhang, B. Yang, L. Jiang, *Adv. Mater.* **2007**, *19*, 2213 – 2217.
[8] S. Kinoshita, S. Yoshioka, *ChemPhysChem* **2005**, *6*, 1442 – 1459.

[9] F. Marlow, Muldarisnur, P. Sharifi, R. Brinkmann, C. Mendive, *Angew. Chem.* **2009**, *121*, 6328 – 6351; *Angew. Chem. Int. Ed.* **2009**, *48*, 6212 – 6233.
[10] A. R. Parker, V. L. Welch, D. Driver, N. Martini, *Nature* **2003**, *426*, 786 – 787.
[11] A. E. Seago, P. Brady, J.-P. Vigneron, T. D. Schultz, *J. R. Soc. Interface* **2009**, *6*, S165 – S184.
[12] H. M. Whitney, M. Kolle, P. Andrew, L. Chittka, U. Steiner, B. J. Glover, *Science* **2009**, *323*, 130 – 133.
[13] S. Vignolini, P. J. Rudall, A. V. Rowland, A. Reed, E. Moyroud, R. B. Faden, J. J. Baumberg, B. J. Glover, U. Steiner, *Proc. Natl. Acad. Sci. USA* **2012**, *109*, 15712 – 15715.
[14] J. D. Joannopoulos, S. G. Johnson, J. N. Winn, R. D. Meade, *Photonic Crystals*: *Molding the Flow of Light*, *2nd ed.*, Princeton University Press, Princeton, **2008**.
[15] E. Yablonovitch, *Phys. Rev. Lett.* **1987**, *58*, 2059 – 2062.
[16] S. John, *Phys. Rev. Lett.* **1987**, *58*, 2486 – 2489.
[17] B. V. Lotsch, G. A. Ozin, *ACS Nano* **2008**, *2*, 2065 – 2074.
[18] B. V. Lotsch, G. A. Ozin, *Adv. Mater.* **2008**, *20*, 4079 – 4084.
[19] Z. Wang, J. Zhang, J. Xie, Y. Yin, Z. Wang, H. Shen, Y. Li, J. Li, S. Liang, S. L. L. Y. Cui, L. Zhang, H. Zhang, B. Yang, *ACS Appl. Mater. Interfaces* **2012**, *4*, 1397 – 1403.
[20] J.-T. Zhang, L. Wang, D. N. Lamont, S. S. Velankar, S. A. Asher, *Angew. Chem.* **2012**, *124*, 6221 – 6224; *Angew. Chem. Int. Ed.* **2012**, *51*, 6117 – 6120.
[21] J. Ge, Y. Yin, *Angew. Chem.* **2011**, *123*, 1530 – 1561; *Angew. Chem. Int. Ed.* **2011**, *50*, 1492 – 1522.
[22] T. F. Krauss, R. M. D. L. Rue, S. Brand, *Nature* **1996**, *383*, 699 – 702.
[23] O. Painter, R. K. Lee, A. Scherer, A. Yariv, J. D. O'Brien, P. D. Dapkus, I. Kim, *Science* **1999**, *284*, 1819 – 1821.
[24] H. Benisty, C. Weisbuch, D. Labilloy, M. Rattier, C. J. M. Smith, T. F. Krauss, R. M. De La Rue, R. Houdre, U. Oesterle, C. Jouanin, D. Cassagne, *J. Lightwave Technol.* **1999**, *17*, 2063 – 2077.
[25] S. Noda, A. Chutinan, M. Imada, *Nature* **2000**, *407*, 608 – 610.
[26] J.-T. Zhang, L. Wang, X. Chao, S. S. Velankar, S. A. Asher, *J. Mater. Chem. C* **2013**, *1*, 6099 – 6102.
[27] J.-T. Zhang, X. Chao, X. Liu, S. A. Asher, *Chem. Commun.* **2013**, *49*, 6337 – 6339.
[28] R. Laghaei, S. A. Asher, R. D. Coalson, *J. Phys. Chem. B* **2013**, *117*, 5271 – 5279.
[29] A. Tikhonov, N. Kornienko, J.-T. Zhang, L. Wang, S. A. Asher, *J. Nanophotonics* **2012**, *6*, 063509.
[30] J. A. Kelly, A. M. Shukaliak, C. C. Y. Cheung, K. E. Shopsowitz, W. Y. Hamad, M. J. MacLachlan, *Angew. Chem.* **2013**, *125*, 9080 – 9084; *Angew. Chem. Int. Ed.* **2013**, *52*, 8912 – 8916.
[31] M. K. Khan, M. Giese, M. Yu, J. A. Kelly, W. Y. Hamad, M. J. MacLachlan, *Angew. Chem.* **2013**, *125*, 9089 – 9092; *Angew. Chem. Int. Ed.* **2013**, *52*, 8921 – 8924.
[32] A. Stein, B. E. Wilson, S. G. Rudisill, *Chem. Soc. Rev.* **2013**, *42*, 2763 – 2803.
[33] S. Y. Lin, J. G. Fleming, D. L. Hetherington, B. K. Smith, R. Biswas, K. M. Ho, M. M. Sigalas, W. Zubrzycki, S. R. Kurtz, J. Bur, *Nature* **1998**, *394*, 251 – 253.
[34] J. G. Fleming, S.-Y. Lin, *Opt. Lett.* **1999**, *24*, 49 – 51.
[35] S. Noda, K. Tomoda, N. Yamamoto, A. Chutinan, *Science* **2000**, *289*, 604 – 606.
[36] S. Ogawa, M. Imada, S. Yoshimoto, M. Okano, S. Noda, *Science* **2004**, *305*, 227 – 229.
[37] Z. Yang, S. Gao, W. Li, V. Vlasko-Vlasov, U. Welp, W.-K. Kwok, T. Xu, *ACS Appl. Mater. Interfaces* **2011**, *3*, 1101 – 1108.
[38] G. von Freymann, V. Kitaev, B. V. Lotsch, G. A. Ozin, *Chem. Soc. Rev.* **2013**, *42*, 2528 – 2554.
[39] H. Cong, B. Yu, J. Tang, Z. Li, X. Liu, *Chem. Soc. Rev.* **2013**, *42*, 7774 – 7800.
[40] Z. Yu, C.-F. Wang, L. Ling, L. Chen, S. Chen, *Angew. Chem.* **2012**, *124*, 2425 – 2428; *Angew. Chem. Int. Ed.* **2012**, *51*, 2375 – 2378.
[41] F. Li, D. P. Josephson, A. Stein, *Angew. Chem.* **2011**, *123*, 378 – 409; *Angew. Chem. Int. Ed.* **2011**, *50*, 360 – 388.
[42] Y. Xia, B. Gates, Y. Yin, Y. Lu, *Adv. Mater.* **2000**, *12*, 693 – 713.
[43] R. K. Iler, *The Chemistry of Silica*: *Solubility*, *Polymerization*, *Colloid and Surface Properties*, *and Biochemistry*, Wiley, New York, **1979**.
[44] W. Stöber, A. Fink, E. Bohn, *J. Colloid Interface Sci.* **1968**, *26*, 62 – 69.
[45] E. Matijevic, *Langmuir* **1994**, *10*, 8 – 16.
[46] S. h. Im, Y. t. Lim, D. j. Suh, O. O. Park, *Adv. Mater.* **2002**, *14*, 1367 – 1369.
[47] Y. Nishijima, K. Ueno, S. Juodkazis, V. Mizeikis, H. Misawa, T. Tanimura, K. Maeda, *Opt. Express* **2007**, *15*, 12979 – 12988.
[48] C. I. Aguirre, E. Reguera, A. Stein, *ACS Appl. Mater. Interfaces* **2010**, *2*, 3257 – 3262.
[49] Z. Cai, Y. J. Liu, J. Teng, X. Lu, *ACS Appl. Mater. Interfaces* **2012**, *4*, 5562 – 5569.
[50] R. J. Carlson, S. A. Asher, *Appl. Spectrosc.* **1984**, *38*, 297 – 304.
[51] S. A. Asher, P. L. Flaugh, G. Washinger, *Spectroscopy* **1986**, *1*, 26 – 31.
[52] P. Pieranski, *Contemp. Phys.* **1983**, *24*, 25 – 73.
[53] W. Van Negen, I. Shook, *Adv. Colloid Interface Sci.* **1984**, *21*, 119 – 194.
[54] W. Massa, *Kristallstrukturbestimmung*, Vieweg Teubner/Springer, Wiesbaden, **2011**.
[55] H. Fudouzi, *J. Colloid Interface Sci.* **2004**, *275*, 277 – 283.
[56] Y.-J. Lee, P. V. Braun, *Adv. Mater.* **2003**, *15*, 563 – 566.
[57] C. I. Aguirre, E. Reguera, A. Stein, *Adv. Funct. Mater.* **2010**, *20*, 2565 – 2578.
[58] H. Wang, K.-Q. Zhang, *Sensors* **2013**, *13*, 4192 – 4213.
[59] S.-H. Kim, S.-J. Jeon, W. C. Jeong, H. S. Park, S.-M. Yang, *Adv. Mater.* **2008**, *20*, 4129 – 4134.
[60] J. Ge, H. Lee, L. He, J. Kim, Z. Lu, H. Kim, J. Goebl, S. Kwon, Y. Yin, *J. Am. Chem. Soc.* **2009**, *131*, 15687 – 15694.
[61] V. N. Konopsky, E. V. Alieva, *Anal. Chem.* **2007**, *79*, 4729 – 4735.
[62] H. Saito, Y. Takeoka, M. Watanabe, *Chem. Commun.* **2003**, 2126 – 2127.
[63] M. G. Scullion, A. Di Falco, T. F. Krauss, *Biosens. Bioelectron.* **2011**, *27*, 101 – 105.
[64] J. B. Jensen, L. H. Pedersen, P. E. Hoiby, L. B. Nielsen, T. P. Hansen, J. R. Folkenberg, J. Riishede, D. Noordegraaf, K. Nielsen, A. Carlsen, A. Bjarklev, *Opt. Lett.* **2004**, *29*, 1974 – 1976.
[65] S. Mandal, J. M. Goddard, D. Erickson, *Lab Chip* **2009**, *9*, 2924 – 2932.
[66] S. Arnold, D. Keng, S. I. Shopova, S. Holler, W. Zurawsky, F. Vollmer, *Opt. Express* **2009**, *17*, 6230 – 6238.
[67] D. K. Armani, T. J. Kippenberg, S. M. Spillane, K. J. Vahala, *Nature* **2003**, *421*, 925 – 928.
[68] J. Vučković, M. Lončar, H. Mabuchi, A. Scherer, *Phys. Rev. E* **2001**, *65*, 016608.
[69] D. Mori, T. Baba, *Opt. Express* **2005**, *13*, 9398 – 9408.
[70] M. M. Orosco, C. Pacholski, M. J. Sailor, *Nat. Nanotechnol.* **2009**, *4*, 255 – 258.
[71] L. D. Bonifacio, D. P. Puzzo, S. Breslav, B. M. Willey, A. McGeer, G. A. Ozin, *Adv. Mater.* **2010**, *22*, 1351 – 1354.
[72] S. Colodrero, M. Ocana, H. Miguez, *Langmuir* **2008**, *24*, 4430 – 4434.
[73] R. A. Potyrailo, Z. Ding, M. D. Butts, S. E. Genovese, T. Deng, *IEEE Sens. J.* **2008**, *8*, 815 – 822.
[74] K. Lee, S. A. Asher, *J. Am. Chem. Soc.* **2000**, *122*, 9534 – 9537.

[75] S. A. Asher, V. L. Alexeev, A. V. Goponenko, A. C. Sharma, I. K. Lednev, C. S. Wilcox, D. N. Finegold, *J. Am. Chem. Soc.* **2003**, *125*, 3322 – 3329.
[76] X. Xu, A. V. Goponenko, S. A. Asher, *J. Am. Chem. Soc.* **2008**, *130*, 3113 – 3119.
[77] Z.-Z. Gu, A. Fujishima, O. Sato, *J. Am. Chem. Soc.* **2000**, *122*, 12387 – 12388.
[78] S. Kubo, Z.-Z. Gu, K. Takahashi, Y. Ohko, O. Sato, A. Fujishima, *J. Am. Chem. Soc.* **2002**, *124*, 10950 – 10951.
[79] S. Kubo, Z.-Z. Gu, K. Takahashi, A. Fujishima, H. Segawa, O. Sato, *J. Am. Chem. Soc.* **2004**, *126*, 8314 – 8319.
[80] H. Fudouzi, Y. Xia, *Adv. Mater.* **2003**, *15*, 892 – 896.
[81] H. Fudouzi, Y. Xia, *Langmuir* **2003**, *19*, 9653 – 9660.
[82] C. Fenzl, T. Hirsch, O. Wolfbeis, *Sensors* **2012**, *12*, 16954 – 16963.
[83] C. Fenzl, S. Wilhelm, T. Hirsch, O. S. Wolfbeis, *ACS Appl. Mater. Interfaces* **2013**, *5*, 173 – 178.
[84] A. C. Arsenault, T. J. Clark, G. von Freymann, L. Cademartiri, R. Sapienza, J. Bertolotti, E. Vekris, S. Wong, V. Kitaev, I. Manners, R. Z. Wang, S. John, D. Wiersma, G. A. Ozin, *Nat. Mater.* **2006**, *5*, 179 – 184.
[85] J. Li, Y. Wu, J. Fu, Y. Cong, J. Peng, Y. Han, *Chem. Phys. Lett.* **2004**, *390*, 285 – 289.
[86] I. B. Burgess, M. Lončar, J. Aizenberg, *J. Mater. Chem. C* **2013**, *1*, 6075 – 6086.
[87] S. A. Asher, J. Holtz, L. Liu, Z. Wu, *J. Am. Chem. Soc.* **1994**, *116*, 4997 – 4998.
[88] J. M. Jethmalani, W. T. Ford, *Chem. Mater.* **1996**, *8*, 2138 – 2146.
[89] S. H. Foulger, P. Jiang, A. C. Lattam, D. W. Smith, J. Ballato, *Langmuir* **2001**, *17*, 6023 – 6026.
[90] S. H. Foulger, P. Jiang, A. Lattam, D. W. Smith, J. Ballato, D. E. Dausch, S. Grego, B. R. Stoner, *Adv. Mater.* **2003**, *15*, 685 – 689.
[91] X. Wang, O. S. Wolfbeis, R. J. Meier, *Chem. Soc. Rev.* **2013**, *42*, 7834 – 7869.
[92] J. M. Weissman, H. B. Sunkara, A. S. Tse, S. A. Asher, *Science* **1996**, *274*, 959 – 963.
[93] J. D. Debord, L. A. Lyon, *J. Phys. Chem. B* **2000**, *104*, 6327 – 6331.
[94] Z. Hu, X. Lu, J. Gao, *Adv. Mater.* **2001**, *13*, 1708 – 1712.
[95] C. E. Reese, A. V. Mikhonin, M. Kamenjicki, A. Tikhonov, S. A. Asher, *J. Am. Chem. Soc.* **2004**, *126*, 1493 – 1496.
[96] M. C. Chiappelli, R. C. Hayward, *Adv. Mater.* **2012**, *24*, 6100 – 6104.
[97] Y. Hu, J. Wang, H. Wang, Q. Wang, J. Zhu, Y. Yang, *Langmuir* **2012**, *28*, 17186 – 17192.
[98] G. Wu, Y. Jiang, D. Xu, H. Tang, X. Liang, G. Li, *Langmuir* **2011**, *27*, 1505 – 1509.
[99] J. Ballato, A. James, *J. Am. Ceram. Soc.* **1999**, *82*, 2273 – 2275.
[100] Y. Takeoka, M. Watanabe, *Langmuir* **2003**, *19*, 9104 – 9106.
[101] M. Kumoda, M. Watanabe, Y. Takeoka, *Langmuir* **2006**, *22*, 4403 – 4407.
[102] T. Dey, *J. Sol-Gel Sci. Technol.* **2011**, *57*, 132 – 141.
[103] M. Honda, T. Seki, Y. Takeoka, *Adv. Mater.* **2009**, *21*, 1801 – 1804.
[104] U. Jeong, Y. Xia, *Angew. Chem.* **2005**, *117*, 3159 – 3163; *Angew. Chem. Int. Ed.* **2005**, *44*, 3099 – 3103.
[105] A. B. Pevtsov, D. A. Kurdyukov, V. G. Golubev, A. V. Akimov, A. A. Meluchev, A. V. Sel′kin, A. A. Kaplyanskii, D. R. Yakovlev, M. Bayer, *Phys. Rev. B* **2007**, *75*, 153101.
[106] J. Zhou, C. Q. Sun, K. Pita, Y. L. Lam, Y. Zhou, S. L. Ng, C. H. Kam, L. T. Li, Z. L. Gui, *Appl. Phys. Lett.* **2001**, *78*, 661 – 663.
[107] N. Tétreault, H. Míguez, S. m. Yang, V. Kitaev, G. A. Ozin, *Adv. Mater.* **2003**, *15*, 1167 – 1172.
[108] A. T. Exner, I. Pavlichenko, B. V. Lotsch, G. Scarpa, P. Lugli, *ACS Appl. Mater. Interfaces* **2013**, *5*, 1575 – 1582.
[109] M. Kamenjicki, I. K. Lednev, A. Mikhonin, R. Kesavamoorthy, S. A. Asher, *Adv. Funct. Mater.* **2003**, *13*, 774 – 780.
[110] M. K. Maurer, I. K. Lednev, S. A. Asher, *Adv. Funct. Mater.* **2005**, *15*, 1401 – 1406.
[111] K. Hwang, D. Kwak, C. Kang, D. Kim, Y. Ahn, Y. Kang, *Angew. Chem.* **2011**, *123*, 6435 – 6438; *Angew. Chem. Int. Ed.* **2011**, *50*, 6311 – 6314.
[112] Y. Shimoda, M. Ozaki, K. Yoshino, *Appl. Phys. Lett.* **2001**, *79*, 3627 – 3629.
[113] M. Ozaki, Y. Shimoda, M. Kasano, K. Yoshino, *Adv. Mater.* **2002**, *14*, 514 – 518.
[114] A. C. Arsenault, H. Míguez, V. Kitaev, G. A. Ozin, I. Manners, *Adv. Mater.* **2003**, *15*, 503 – 507.
[115] A. C. Arsenault, D. P. Puzzo, I. Manners, G. A. Ozin, *Nat. Photonics* **2007**, *1*, 468 – 472.
[116] D. P. Puzzo, A. C. Arsenault, I. Manners, G. A. Ozin, *Angew. Chem.* **2009**, *121*, 961 – 965; *Angew. Chem. Int. Ed.* **2009**, *48*, 943 – 947.
[117] K. Ueno, K. Matsubara, M. Watanabe, Y. Takeoka, *Adv. Mater.* **2007**, *19*, 2807 – 2812.
[118] K. Ueno, J. Sakamoto, Y. Takeoka, M. Watanabe, *J. Mater. Chem.* **2009**, *19*, 4778 – 4783.
[119] Y. Saado, M. Golosovsky, D. Davidov, A. Frenkel, *Phys. Rev. B* **2002**, *66*, 195108.
[120] S. Sacanna, A. P. Philipse, *Langmuir* **2006**, *22*, 10209 – 10216.
[121] C. Zhu, L. Chen, H. Xu, Z. Gu, *Macromol. Rapid Commun.* **2009**, *30*, 1945 – 1949.
[122] X. Xu, G. Friedman, K. D. Humfeld, S. A. Majetich, S. A. Asher, *Adv. Mater.* **2001**, *13*, 1681 – 1684.
[123] X. Xu, G. Friedman, K. D. Humfeld, S. A. Majetich, S. A. Asher, *Chem. Mater.* **2002**, *14*, 1249 – 1256.
[124] J. Ge, Y. Hu, M. Biasini, W. P. Beyermann, Y. Yin, *Angew. Chem.* **2007**, *119*, 4420 – 4423; *Angew. Chem. Int. Ed.* **2007**, *46*, 4342 – 4345.
[125] J. Ge, Y. Hu, Y. Yin, *Angew. Chem.* **2007**, *119*, 7572 – 7575; *Angew. Chem. Int. Ed.* **2007**, *46*, 7428 – 7431.
[126] J. Ren, S. Song, A. Lopez-Valdivieso, J. Shen, S. Lu, *J. Colloid Interface Sci.* **2001**, *238*, 279 – 284.
[127] J. Ge, Y. Yin, *Adv. Mater.* **2008**, *20*, 3485 – 3491.
[128] J. Ge, Y. Yin, *J. Mater. Chem.* **2008**, *18*, 5041 – 5045.
[129] X. Xu, S. A. Majetich, S. A. Asher, *J. Am. Chem. Soc.* **2002**, *124*, 13864 – 13868.
[130] Y. Zhao, Y.-N. Zhang, Q. Wang, *Sens. Actuators B* **2011**, *160*, 1288 – 1297.
[131] V. N. Bogomolov, S. V. Gaponenko, I. N. Germanenko, A. M. Kapitonov, E. P. Petrov, N. V. Gaponenko, A. V. Prokofiev, A. N. Ponyavina, N. I. Silvanovich, S. M. Samoilovich, *Phys. Rev. E* **1997**, *55*, 7619 – 7625.
[132] C. F. Blanford, R. C. Schroden, M. Al-Daous, A. Stein, *Adv. Mater.* **2001**, *13*, 26 – 29.
[133] I. B. Burgess, N. Koay, K. P. Raymond, M. Kolle, M. Lončar, J. Aizenberg, *ACS Nano* **2012**, *6*, 1427 – 1437.
[134] K. P. Raymond, I. B. Burgess, M. H. Kinney, M. Lončar, J. Aizenberg, *Lab Chip* **2012**, *12*, 3666 – 3669.
[135] M. C. Fuertes, F. J. López-Alcaraz, M. C. Marchi, H. E. Troiani, V. Luca, H. Míguez, G. J. D. A. Soler-Illia, *Adv. Funct. Mater.* **2007**, *17*, 1247 – 1254.
[136] S. Y. Choi, M. Mamak, G. von Freymann, N. Chopra, G. A. Ozin, *Nano Lett.* **2006**, *6*, 2456 – 2461.
[137] K. Yao, Y. Shi, *Opt. Express* **2012**, *20*, 27039 – 27044.
[138] R. B. M. Schasfoort, A. J. Tudos, *Handbook of Surface Plasmon Resonance*, Royal Society Of Chemistry, Cambridge, **2008**.
[139] S. Colodrero, M. Ocaña, A. R. González-Elipe, H. Míguez, *Langmuir* **2008**, *24*, 9135 – 9139.
[140] Z. Xie, K. Cao, Y. Zhao, L. Bai, H. Gu, H. Xu, Z. Z. Gu, *Adv. Mater.* **2014**, DOI: 10.1002/adma.201304775.
[141] Y. Dou, J. Han, T. Wang, M. Wei, D. G. Evans, X. Duan, *J. Mater. Chem.* **2012**, *22*, 14001 – 14007.

[142] B. H. King, A. M. Ruminski, J. L. Snyder, M. J. Sailor, *Adv. Mater.* **2007**, *19*, 4530 – 4534.
[143] A. M. Ruminski, B. H. King, J. Salonen, J. L. Snyder, M. J. Sailor, *Adv. Funct. Mater.* **2010**, *20*, 2874 – 2883.
[144] B. H. King, T. Wong, M. J. Sailor, *Langmuir* **2011**, *27*, 8576 – 8585.
[145] J. Dorvee, M. J. Sailor, *Phys. Status Solidi* **2005**, *202*, 1619 – 1623.
[146] T. L. Kelly, A. G. Sega, M. J. Sailor, *Nano Lett.* **2011**, *11*, 3169 – 3173.
[147] C. M. Thompson, A. M. Ruminski, A. G. Sega, M. J. Sailor, G. M. Miskelly, *Langmuir* **2011**, *27*, 8967 – 8973.
[148] F. M. Hinterholzinger, A. Ranft, J. M. Feckl, B. Rühle, T. Bein, B. V. Lotsch, *J. Mater. Chem.* **2012**, *22*, 10356 – 10362.
[149] Y. Huang, G. Pandraud, P. M. Sarro, *Opt. Lett.* **2012**, *37*, 3162 – 3164.
[150] X. Ye, Y. Li, J. Dong, J. Xiao, Y. Ma, L. Qi, *J. Mater. Chem. C* **2013**, *1*, 6112 – 6119.
[151] R. A. Potyrailo, H. Ghiradella, A. Vertiatchikh, K. Dovidenko, J. R. Cournoyer, E. Olson, *Nat. Photonics* **2007**, *1*, 123 – 128.
[152] M. M. Hawkeye, M. J. Brett, *Adv. Funct. Mater.* **2011**, *21*, 3652 – 3658.
[153] I. G. Kolobov, W. B. Euler, I. A. Levitsky, *Appl. Opt.* **2010**, *49*, 137 – 141.
[154] I. Pavlichenko, A. T. Exner, M. Guehl, P. Lugli, G. Scarpa, B. V. Lotsch, *J. Phys. Chem. C* **2012**, *116*, 298 – 305.
[155] A. M. Ruminski, G. Barillaro, C. Chaffin, M. J. Sailor, *Adv. Funct. Mater.* **2011**, *21*, 1511 – 1525.
[156] Y. Kang, J. J. Walish, T. Gorishnyy, E. L. Thomas, *Nat. Mater.* **2007**, *6*, 957 – 960.
[157] T. Endo, Y. Yanagida, T. Hatsuzawa, *Sens. Actuators B* **2007**, *125*, 589 – 595.
[158] Z. Pan, J. Ma, J. Yan, M. Zhou, J. Gao, *J. Mater. Chem.* **2012**, *22*, 2018 – 2025.
[159] Z. Wang, J. Zhang, J. Li, J. Xie, Y. Li, S. Liang, Z. Tian, C. Li, Z. Wang, T. Wang, H. Zhang, B. Yang, *J. Mater. Chem.* **2011**, *21*, 1264 – 1270.
[160] Y. Y. Li, F. Cunin, J. R. Link, T. Gao, R. E. Betts, S. H. Reiver, V. Chin, S. N. Bhatia, M. J. Sailor, *Science* **2003**, *299*, 2045 – 2047.
[161] H. Yang, P. Jiang, B. Jiang, *J. Colloid Interface Sci.* **2012**, *370*, 11 – 18.
[162] I. B. Burgess, L. Mishchenko, B. D. Hatton, M. Kolle, M. Lončar, J. Aizenberg, *J. Am. Chem. Soc.* **2011**, *133*, 12430 – 12432.
[163] G. I. N. Waterhouse, J. B. Metson, H. Idriss, D. Sun-Waterhouse, *Chem. Mater.* **2008**, *20*, 1183 – 1190.
[164] Z. Cai, Y. J. Liu, X. Lu, J. Teng, *J. Phys. Chem. C* **2013**, *117*, 9440 – 9445.
[165] Y. Wu, F. Li, W. Zhu, J. Cui, C. Tao, C. Lin, P. M. Hannam, G. Li, *Angew. Chem.* **2011**, *123*, 12726 – 12730; *Angew. Chem. Int. Ed.* **2011**, *50*, 12518 – 12522.
[166] N. Kumano, T. Seki, M. Ishii, H. Nakamura, Y. Takeoka, *Angew. Chem.* **2011**, *123*, 4098 – 4101; *Angew. Chem. Int. Ed.* **2011**, *50*, 4012 – 4015.
[167] E. Tian, J. Wang, Y. Zheng, Y. Song, L. Jiang, D. Zhu, *J. Mater. Chem.* **2008**, *18*, 1116 – 1122.
[168] R. Xuan, Q. Wu, Y. Yin, J. Ge, *J. Mater. Chem.* **2011**, *21*, 3672 – 3676.
[169] J. Huang, C. Tao, Q. An, C. Lin, X. Li, D. Xu, Y. Wu, X. Li, D. Shen, G. Li, *Chem. Commun.* **2010**, *46*, 4103 – 4105.
[170] H. Hu, Q.-W. Chen, K. Cheng, J. Tang, *J. Mater. Chem.* **2012**, *22*, 1021 – 1027.
[171] L. Wang, J. Wang, Y. Huang, M. Liu, M. Kuang, Y. Li, L. Jiang, Y. Song, *J. Mater. Chem.* **2012**, *22*, 21405 – 21411.
[172] H. Li, L. Chang, J. Wang, L. Yang, Y. Song, *J. Mater. Chem.* **2008**, *18*, 5098 – 5103.
[173] C. Li, B. V. Lotsch, *Chem. Commun.* **2012**, *48*, 6169 – 6171.
[174] J.-T. Zhang, L. Wang, J. Luo, A. Tikhonov, N. Kornienko, S. A. Asher, *J. Am. Chem. Soc.* **2011**, *133*, 9152 – 9155.
[175] S. A. Asher, K. W. Kimble, J. P. Walker, *Chem. Mater.* **2008**, *20*, 7501 – 7509.
[176] Q. Yang, S. Zhu, W. Peng, C. Yin, W. Wang, J. Gu, W. Zhang, J. Ma, T. Deng, C. Feng, D. Zhang, *ACS Nano* **2013**, *7*, 4911 – 4918.
[177] M. Chen, L. Zhou, Y. Guan, Y. Zhang, *Angew. Chem. Int. Ed.* **2013**, *52*, 9961 – 9965.
[178] C. Chen, Y. Zhu, H. Bao, J. Shen, H. Jiang, L. Peng, X. Yang, C. Li, G. Chen, *Chem. Commun.* **2011**, *47*, 5530 – 5532.
[179] S. A. Asher, A. C. Sharma, A. V. Goponenko, M. M. Ward, *Anal. Chem.* **2003**, *75*, 1676 – 1683.
[180] F. Yan, S. Asher, *Anal. Bioanal. Chem.* **2007**, *387*, 2121 – 2130.
[181] See Ref. [62].
[182] J. H. Holtz, S. A. Asher, *Nature* **1997**, *389*, 829 – 832.
[183] J. H. Holtz, J. S. W. Holtz, C. H. Munro, S. A. Asher, *Anal. Chem.* **1998**, *70*, 780 – 791.
[184] C. E. Reese, S. A. Asher, *Anal. Chem.* **2003**, *75*, 3915 – 3918.
[185] A. V. Goponenko, S. A. Asher, *J. Am. Chem. Soc.* **2005**, *127*, 10753 – 10759.
[186] M. M. W. Muscatello, S. A. Asher, *Adv. Funct. Mater.* **2008**, *18*, 1186 – 1193.
[187] H. Jiang, Y. Zhu, C. Chen, J. Shen, H. Bao, L. Peng, X. Yang, C. Li, *New J. Chem.* **2012**, *36*, 1051 – 1056.
[188] X. Hu, J. Huang, W. Zhang, M. Li, C. Tao, G. Li, *Adv. Mater.* **2008**, *20*, 4074 – 4078.
[189] C. Ma, Y. Jiang, X. Yang, C. Wang, H. Li, F. Dong, B. Yang, K. Yu, Q. Lin, *ACS Appl. Mater. Interfaces* **2013**, *5*, 1990 – 1996.
[190] J.-T. Zhang, N. Smith, S. A. Asher, *Anal. Chem.* **2012**, *84*, 6416 – 6420.
[191] X. Hu, G. Li, J. Huang, D. Zhang, Y. Qiu, *Adv. Mater.* **2007**, *19*, 4327 – 4332.
[192] N. Griffete, H. Frederich, A. Maître, C. Schwob, S. Ravaine, B. Carbonnier, M. M. Chehimi, C. Mangeney, *J. Colloid Interface Sci.* **2011**, *364*, 18 – 23.
[193] C. Guo, C. Zhou, N. Sai, B. Ning, M. Liu, H. Chen, Z. Gao, *Sens. Actuators B* **2012**, *166 – 167*, 17 – 23.
[194] J. Li, Z. Zhang, S. Xu, L. Chen, N. Zhou, H. Xiong, H. Peng, *J. Mater. Chem.* **2011**, *21*, 19267 – 19274.
[195] H. Peng, S. Wang, Z. Zhang, H. Xiong, J. Li, L. Chen, Y. Li, *J. Agric. Food Chem.* **2012**, *60*, 1921 – 1928.
[196] Y. Yuan, Z. Li, Y. Liu, J. Gao, Z. Pan, Y. Liu, *Chem. Eur. J.* **2012**, *18*, 303 – 309.
[197] Y.-X. Zhang, P.-Y. Zhao, L.-P. Yu, *Sens. Actuators B* **2013**, *181*, 850 – 857.
[198] K. W. Kimble, J. P. Walker, D. N. Finegold, S. A. Asher, *Anal. Bioanal. Chem.* **2006**, *385*, 678 – 685.
[199] C. Liu, G. Gao, Y. Zhang, L. Wang, J. Wang, Y. Song, *Macromol. Rapid Commun.* **2012**, *33*, 380 – 385.
[200] H. S. Mader, O. S. Wolfbeis, *Microchim. Acta* **2008**, *162*, 1 – 34.
[201] M. Ben-Moshe, V. L. Alexeev, S. A. Asher, *Anal. Chem.* **2006**, *78*, 5149 – 5157.
[202] V. L. Alexeev, S. Das, D. N. Finegold, S. A. Asher, *Clin. Chem.* **2004**, *50*, 2353 – 2360.
[203] V. L. Alexeev, A. C. Sharma, A. V. Goponenko, S. Das, I. K. Lednev, C. S. Wilcox, D. N. Finegold, S. A. Asher, *Anal. Chem.* **2003**, *75*, 2316 – 2323.
[204] O. B. Ayyub, M. B. Ibrahim, R. M. Briber, P. Kofinas, *Biosens. Bioelectron.* **2013**, *46*, 124 – 129.
[205] Y. Zhao, X. Zhao, Z. Gu, *Adv. Funct. Mater.* **2010**, *20*, 2970 – 2988.
[206] A. C. Sharma, T. Jana, R. Kesavamoorthy, L. Shi, M. A. Virji, D. N. Finegold, S. A. Asher, *J. Am. Chem. Soc.* **2004**, *126*, 2971 – 2977.

[207] M. K. Maurer, S. E. Gould, P. J. Scott, *Sens. Actuators B* **2008**, *134*, 736 – 742.
[208] J. P. Walker, S. A. Asher, *Anal. Chem.* **2005**, *77*, 1596 – 1600.
[209] J. P. Walker, K. W. Kimble, S. A. Asher, *Anal. Bioanal. Chem.* **2007**, *389*, 2115 – 2124.
[210] C. Preininger, O. S. Wolfbeis, *Biosens. Bioelectron.* **1996**, *11*, 981 – 990.
[211] D. Arunbabu, A. Sannigrahi, T. Jana, *Soft Matter* **2011**, *7*, 2592 – 2599.
[212] M. Liu, L.-P. Yu, *Analyst* **2013**, *138*, 3376 – 3379.
[213] Y. Guo, J. Y. Ye, C. Divin, B. Huang, T. P. Thomas, J. Baker, T. B. Norris, *Anal. Chem.* **2010**, *82*, 5211 – 5218.
[214] P. Rivolo, F. Michelotti, F. Frascella, G. Digregorio, P. Mandracci, L. Dominici, F. Giorgis, E. Descrovi, *Sens. Actuators B* **2012**, *161*, 1046 – 1052.
[215] M. Li, F. He, Q. Liao, J. Liu, L. Xu, L. Jiang, Y. Song, S. Wang, D. Zhu, *Angew. Chem.* **2008**, *120*, 7368 – 7372; *Angew. Chem. Int. Ed.* **2008**, *47*, 7258 – 7262.
[216] T. J. Park, S.-K. Lee, S. M. Yoo, S.-M. Yang, S. Y. Lee, *J. Nanosci. Nanotechnol.* **2011**, *11*, 632 – 637.
[217] F. Fleischhaker, A. C. Arsenault, F. C. Peiris, V. Kitaev, I. Manners, R. Zentel, G. A. Ozin, *Adv. Mater.* **2006**, *18*, 2387 – 2391.
[218] B.-F. Ye, Y.-J. Zhao, Y. Cheng, T.-T. Li, Z.-Y. Xie, X.-W. Zhao, Z.-Z. Gu, *Nanoscale* **2012**, *4*, 5998 – 6003.
[219] M. R. Lee, P. M. Fauchet, *Opt. Express* **2007**, *15*, 4530 – 4535.
[220] I. D. Block, L. L. Chan, B. T. Cunningham, *Sens. Actuators B* **2006**, *120*, 187 – 193.
[221] J.-H. Han, H.-J. Kim, L. Sudheendra, S. J. Gee, B. D. Hammock, I. M. Kennedy, *Anal. Chem.* **2013**, *85*, 3104 – 3109.
[222] J. Escorihuela, M. J. Bañuls, J. G. Castelló, V. Toccafondo, J. García-Rupérez, R. Puchades, Á. Maquieira, *Anal. Bioanal. Chem.* **2012**, *404*, 2831 – 2840.
[223] T. Endo, C. Ueda, H. Kajita, N. Okuda, S. Tanaka, H. Hisamoto, *Microchim. Acta* **2013**, *180*, 929 – 934.
[224] T. Endo, M. Sato, H. Kajita, N. Okuda, S. Tanaka, H. Hisamoto, *Lab Chip* **2012**, *12*, 1995 – 1999.
[225] B. Guan, A. Magenau, K. A. Kilian, S. Ciampi, K. Gaus, P. J. Reece, J. J. Gooding, *Faraday Discuss.* **2011**, *149*, 301 – 317.
[226] J. Li, X. Zhao, H. Wei, Z.-Z. Gu, Z. Lu, *Anal. Chim. Acta* **2008**, *625*, 63 – 69.
[227] X. Zhao, Y. Cao, F. Ito, H.-H. Chen, K. Nagai, Y.-H. Zhao, Z.-Z. Gu, *Angew. Chem.* **2006**, *118*, 6989 – 6992; *Angew. Chem. Int. Ed.* **2006**, *45*, 6835 – 6838.
[228] G. Deng, K. Xu, Y. Sun, Y. Chen, T. Zheng, J. Li, *Anal. Chem.* **2013**, *85*, 2833 – 2840.
[229] J. O. Grepstad, P. Kaspar, O. Solgaard, I.-R. Johansen, A. S. Sudbø, *Opt. Express* **2012**, *20*, 7954 – 7965.
[230] O. S. Wolfbeis, *Angew. Chem.* **2013**, *125*, 10048 – 10049; *Angew. Chem. Int. Ed.* **2013**, *52*, 9864 – 9865.
[231] G. A. Ozin, A. C. Arsenault, *Mater. Today* **2008**, *11*, 44 – 51.
[232] J. T. Heeres, P. J. Hergenrother, *Chem. Soc. Rev.* **2011**, *40*, 4398 – 4410.
[233] M. Fujishima, S. Sakata, T. Iwasaki, K. Uchida, *J. Mater. Sci.* **2008**, *43*, 1890 – 1896.
[234] R. Badugu, K. Nowaczyk, E. Descrovi, J. R. Lakowicz, *Anal. Biochem.* **2013**, *442*, 83 – 96.